

# Analysis of Mass Flow in Transmutation System with Two-Member Chain

J. Ahn, P. L. Chambré, and B. H. Park

Department of Nuclear Engineering  
University of California, Berkeley  
Berkeley, CA 94720-1730

March 2002

The authors invite comments and would appreciate  
being notified of any errors in the report.

Joonhong Ahn  
Department of Nuclear Engineering  
University of California  
Berkeley, CA 94720  
USA

[ahn@nuc.berkeley.edu](mailto:ahn@nuc.berkeley.edu)

# TABLE OF CONTENTS

<b>1. INTRODUCTION.....</b>	<b>1</b>
<b>2. MODEL FOR TWO-MEMBER CHAINS.....</b>	<b>2</b>
2.1 MATHEMATICAL FORMULATION FOR SIMPLIFIED TRANSMUTATION SYSTEM.....	2
2.1.1 ATW fuel material.....	2
2.1.2 Transmutation.....	2
2.1.3 Treatment of Irradiated ATW Fuel.....	4
2.1.4 Ranges of System Parameters.....	6
2.2 ANALYTICAL SOLUTIONS FOR MULTIPLE CYCLES .....	7
2.2.1 Recursive Solutions for Multiple Cycles.....	7
2.2.2 Non-Recursive Solutions for Multiple Cycles.....	7
(a) Case (I): Recycling Case ( $0 < \alpha < 1$ ).....	9
(b) Case (II): Once-Through Case ( $\alpha = 1$ ).....	11
2.2.3 Asymptotic Behavior of Non-Recursive Solutions for Large Cycle Numbers.....	13
2.3 SOME QUANTITIES OF INTEREST .....	13
2.3.1 Cumulative Fractions of TRU Radionuclides in Waste .....	13
2.3.2 Cumulative Feed of TRU Radionuclides.....	13
2.3.3 Cumulative Fraction of Transmutation Products in Waste.....	14
2.3.4 TRU Reduction Ratio .....	14
2.3.5 Transmutation-Product Ratio .....	15
2.3.6 The Fractional Transmutation .....	16
APPENDIX FOR CHAPTER 2 .....	16
<b>3. NUMERICAL RESULTS AND DISCUSSIONS.....</b>	<b>20</b>
3.1 TIME-DEPENDENT BEHAVIOR .....	20
3.1.1 TRU Radionuclide Fractions (Figure 3-1).....	21
3.1.2 Cumulative Fractions (Figure 3-2).....	22
3.1.3 TRU Reduction Ratios (Figure 3-3).....	22
3.1.4 Transmutation-Product Ratio (Figure 3-4).....	26
3.1.5 Fractional Transmutation (Figure 3-5).....	26
3.2 EFFECTS OF SYSTEM PARAMETERS ON TRU REDUCTION RATIO AT STEADY STATES.....	26
3.2.1 Case with $p_2 = 0$ and $d_1 = d_2 = d$ .....	27
3.2.2 Case with $p_2 = 0.3$ and $d_1 = d_2 = d$ .....	29
<b>4. STABILITY OF THE TWO-MEMBER SYSTEM.....</b>	<b>32</b>
4.1 UPPER BOUNDS OF THE EIGENVALUES .....	32
4.2 EIGENVALUES AND SYSTEM PARAMETERS .....	33
<b>5. CONCLUDING REMARKS .....</b>	<b>37</b>
<b>6. REFERENCES .....</b>	<b>38</b>

## Table of Figures

Figure 2-1:	Schematical diagram for mass flow in the simplified system. Square boxes represent processes, while the boxes with rounded corners represent materials that are derived from or fed into a process. See Eqs. (2.1.1), (2.1.8) and (2.1.20) for the definitions for non-dimensionalized quantities.....	6
Figure 3-1:	Change of radionuclide fractions in the core with the cycle number $i$ . Cases (a) and (b) compare the effects of the destruction coefficient, whereas cases (b) and (c) compare the effects of the production coefficient. ....	23
Figure 3-2:	Cumulative fractions relative to the core. ....	24
Figure 3-3:	TRU reduction ratios for cases (a), (b), and (c). For cases (a) and (b), the reduction ratio is identical for both radionuclides. For case (c), the reduction ratio for the first member is the same as that for case (b).....	25
Figure 3-4:	Transmutation-product ratio for cases (a), (b), and (c). ....	25
Figure 3-5:	Fractional transmutation for cases (a), (b), and (c). For cases (a) and (b), this quantity is identical for both radionuclides.....	26
Figure 3-6:	Dependency of the steady-state TRU reduction ratio on the destruction coefficient, $d$ for $p_2 = 0$ and $d_1 = d_2 = d$ .....	28
Figure 3-7:	Dependency of the steady-state TRU reduction ratio on the combined parameter, $\alpha f$ for $p_2 = 0$ and $d_1 = d_2 = d$ .....	28
Figure 3-8:	Contour plot for the steady-state TRU reduction ratio for $p_2 = 0$ and $d_1 = d_2 = d$ . Two solid-line arrows indicate that both an increase of $d$ by a factor of 10 and a decrease of $\alpha f$ by a factor of 10 give the decrease of the TRU reduction ratio from 0.99 to 0.9. The dashed-line arrows indicate that while the TRU reduction ratio is decreased from 1E-4 to 1E-5 by a decrease of $\alpha f$ by a factor of 10 and an increase of $d$ by a factor of 3.....	29
Figure 3-9:	Dependency of the steady-state TRU reduction ratio on the destruction coefficient, $d$ . ....	30
Figure 3-10:	Dependency of the steady-state TRU reduction ratio on the combined parameter, $\alpha f$ .....	30
Figure 3-11:	Contour plots for the steady-state TRU reduction ratios. The left figure is for the first member, whereas the right is for the second member.....	31
Figure 3-12:	Dependency of the steady-state TRU reduction ratio on the fraction of the first member, $\gamma_1$ . ..	31
Figure 4-1:	Trace of the system matrix as a function of the fraction $f$ for the case with $d_1 = d_2 = 0.05$ and $p_2 = 0$ for different values of $\alpha$ , calculated by (4.1.18).....	35
Figure 4-2:	Trace of the system matrix as a function of the fraction $f$ for the case with $d_1 = d_2 = d$ , $\alpha = 0.003$ , and $p_2 = 0$ , for different values of $d$ , calculated by (4.1.18). ....	35
Figure 4-3:	Trace of the system matrix as a function of the fraction $f$ for the case with $d_1 = d_2 = 0.05$ , $\gamma_1 = 0.635$ , and $p_2 = 0.3$ for different values of $\alpha$ , calculated by (4.1.17). ....	36
Figure 4-4:	Trace of the system matrix as a function of the fraction $f$ for the case with $d_1 = d_2 = d$ , $\alpha = 0.003$ , $\gamma_1 = 0.635$ , and $p_2 = 0.3$ , for different values of $d$ , calculated by (4.1.17). ....	36

## List of Tables

Table I:	Parameter Values Assumed in Reference [3].....	20
Table II:	Values for Non-Dimensionalized Parameters Used in Section 2.4.1, Calculated Values for Matrix Elements and Eigenvalues, and Values for Steady-State Quantities. ....	21
Table III:	Upper-Bound of the Eigenvalues for Cases (a), (b), and (c). ....	33

# 1. INTRODUCTION

This report presents results of a mathematical analysis for mass flow in an accelerator-driven transmutation of waste (ATW) system. A chain of two radionuclides is considered. The present mass flow analysis takes into account change in the composition of radionuclides in the transmuter due to nuclear reactions and the loss of the radionuclides from chemical separation processes.

In the ATW concept [1], transuranic (TRU) radionuclides are recovered by reprocessing of spent fuel from commercial light-water reactors (LWR). The recovered TRU is utilized as fuel materials for a specially-designed subcritical reactor, driven by an accelerator, with which excess neutrons are supplied<sup>1</sup>. Energy liberated by fission reactions in TRU radionuclides is converted to electricity. Thus, TRU materials that are once considered as wastes can be utilized as fuel, and the resultant fission products are expected to be shorter-lived and less toxic than original TRU radionuclides. After irradiation by neutrons in the transmuter core, the fuel for the ATW transmuter, which is made of TRU radionuclides, may still contain considerable amount of TRU radionuclides. Therefore, TRU radionuclides remaining in the irradiated fuel would be partitioned from fission products by pyrochemical processes, and fabricated into a fuel again for further irradiation and transmutation. The TRU radionuclides would be recycled until significant masses of TRU radionuclides are transmuted.

At the reprocessing of LWR spent fuel, at the fabrication of the ATW fuel, and at the partitioning of irradiated ATW fuel, some fractions of those radionuclides are not utilized, and included in the waste. Because one of the objectives of the proposed ATW system is to reduce “impacts”<sup>2</sup> of a geologic repository by reducing the masses of radionuclides in the waste, it is important to estimate the amount of TRU radionuclides included in waste coming from those ATW processes.

The mass flow analysis of the ATW system performed in this study is made by (1) a model for determining the masses of TRU radionuclides in the transmuter as functions of time, which change due to transmutation of TRU, and by (2) a model for determining the composition of the ATW fuel at the beginning of each irradiation period. Between the end of an irradiation period, when the ATW fuel is discharged from the transmuter, and the beginning of the next irradiation period, the partitioning of the TRU radionuclides and the ATW fuel fabrication are assumed to be made instantaneously. The loss of TRU into the waste stream during this period is taken care of by the model (2). TRU radionuclides are assumed to be supplied from the reprocessed LWR spent fuel to make up the mass transmuted in the transmuter and that lost as the waste.

In one of our previous analytical studies [2] for the mass flow analysis, analytical expressions for the fraction of radionuclide mass included in the waste and the fraction of radionuclide mass transmuted after infinitely many cycles were obtained, by assuming that the fractions of radionuclide masses lost as waste and the fraction transmuted by the transmuter do not change from one cycle to another. Change of depletion behavior due to the fuel composition change from one irradiation period to another was neglected. Generation from precursors of a radionuclide by transmutation or by spontaneous decay was neglected.

In the other study [3], an analysis was performed for the evolution of TRU masses in a hypothetical partitioning-transmutation (P-T) system with the 6-member nuclide chain,  $^{238}\text{U}(n,\gamma)^{239}\text{Pu}(n,\gamma)^{240}\text{Pu}(n,\gamma)^{241}\text{Pu}$   
 $\xrightarrow{\beta\text{-decay}} ^{241}\text{Am} \xrightarrow{\alpha\text{-decay}} ^{237}\text{Np}$ . The governing equations for the masses of radionuclides in the transmuter core were established. A *recursive* solution was obtained. The evolution of the masses of the six isotopes in the transmuter were numerically explored.

In the present study, we consider a two-member transmutation chain. A *non-recursive* solution is obtained, which is explicitly written in terms of system parameters. With the non-recursive solution, we define the waste reduction ratio. This ratio is used as a measure for the performance of the recycle system.

---

<sup>1</sup> The accelerator provides high-energy protons to the spallation target to generate the fast neutrons.

<sup>2</sup> This concept is yet to be defined.

## 2. MODEL FOR TWO-MEMBER CHAINS

### 2.1 Mathematical Formulation for Simplified Transmutation System

A simplified transmutation system consists of two main parts: (1) the transmutation and (2) the irradiated fuel treatment (see Figure 2-1).

#### 2.1.1 ATW fuel material

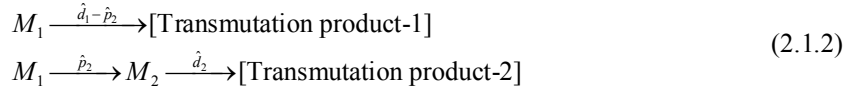
It is assumed that LWR spent fuel has been reprocessed, and a mixture of two TRU radionuclides is already available in the storage for transmutation. The fraction  $\gamma_j, j = 1, 2$ , is defined as the ratio of the number of atoms of radionuclide  $j$  per kg of the mixture of two TRU radionuclides in the storage to the total number of atoms of radionuclides 1 and 2 per kg of the mixture in the storage. The fractions,  $\gamma_1$  and  $\gamma_2$ , for two TRU radionuclides in the storage are assumed to be constant with time. Thus,

$$\gamma_1 + \gamma_2 = 1, 0 < \gamma_1 \leq 1, 0 \leq \gamma_2 < 1. \quad (2.1.1)$$

In Eq. (2.1.1), the case with  $\gamma_1 = 0$  and  $\gamma_2 = 1$  is excluded because there must be the first member in the fuel initially to have a two-member chain. For the first irradiation, the transmuter core contains the fuel consisting of the two TRU radionuclides with fractions,  $\gamma_1$  and  $\gamma_2$ .

#### 2.1.2 Transmutation

The transmuter core is assumed to be uniformized. The composition of the fuel changes with time due to transmutation reactions. Suppose that the first member  $M_1$  is transmuted with the destruction coefficient  $\hat{d}_1$ <sup>3</sup> [yr<sup>-1</sup>]. The transmutation occurs due to the spontaneous decay or the neutron absorption reaction. After neutron absorption, fission or capture reaction would occur. Among transmutation reactions for the first member nuclide  $M_1$ , a certain reaction could generate the second member nuclide  $M_2$  with the production coefficient  $\hat{p}_2$  [yr<sup>-1</sup>]. The second member would be further transmuted with the destruction coefficient  $\hat{d}_2$ . This is depicted as follows:



Generally, between two coefficients, the relation

$$\hat{d}_1 \geq \hat{p}_2. \quad (2.1.3)$$

must be satisfied. If  $\hat{d}_1$  is equal to  $\hat{p}_2$ , then the first member always transmutes to the second member.

For example, consider <sup>241</sup>Pu as the first member, and <sup>241</sup>Am as the second member. Some of <sup>241</sup>Pu changes into <sup>241</sup>Am by a spontaneous beta decay with  $\hat{p}_2$ , while the rest of <sup>241</sup>Pu becomes [Transmutation product-1], something other than <sup>241</sup>Am, by neutron absorption reactions with  $(\hat{d}_1 - \hat{p}_2)$ . In this case,  $\hat{p}_2$  is equal to the radioactive decay constant for the beta decay in <sup>241</sup>Pu. The [Transmutation product-1] includes <sup>242</sup>Pu that is generated by neutron absorption reaction and fission product atoms that are generated by the fission in <sup>241</sup>Pu, whereas the [Transmutation product-2] includes <sup>237</sup>Np generated by alpha decay of <sup>241</sup>Am, <sup>242</sup>Am generated by neutron absorption, and fission product atoms generated by the fission in <sup>241</sup>Am. The transmutation products could be transmuted by further spontaneous decay or neutron absorption reactions, but we do not pursue their evolutions in the present model.

Consider the transmutation of a two-member chain, represented by (2.1.2) in a certain irradiation period. The number of atoms of member  $j$  in the transmuter core at time  $\hat{t}$  is denoted as  $\hat{C}_j(\hat{t})$ . The first member is transmuted at the rate of  $\hat{d}_1 \hat{C}_1(\hat{t})$  [atoms/yr]. Some are transmuted to the second member at the rate of  $\hat{p}_2 \hat{C}_1(\hat{t})$  [atoms/yr]. The second member is transmuted at the rate of  $\hat{d}_2 \hat{C}_2(\hat{t})$ . As time proceeds, the

<sup>3</sup> The ^ symbol stands for the quantity with physical dimensions.

cumulative number<sup>4</sup>  $\hat{C}_p(\hat{t})$  of atoms of the two TRU radionuclides that have been transmuted by the time  $\hat{t}$  increases. The governing equations are written as

$$\begin{aligned}\frac{d\hat{C}_1(\hat{t})}{d\hat{t}} &= -\hat{d}_1\hat{C}_1(\hat{t}), \\ \frac{d\hat{C}_2(\hat{t})}{d\hat{t}} &= -\hat{d}_2\hat{C}_2(\hat{t}) + \hat{p}_2\hat{C}_1(\hat{t}), \quad 0 < \hat{t} < \hat{T}, \quad \hat{d}_1 \geq \hat{p}_2, \\ \frac{d\hat{C}_p(\hat{t})}{d\hat{t}} &= (\hat{d}_1 - \hat{p}_2)\hat{C}_1(\hat{t}) + \hat{d}_2\hat{C}_2(\hat{t}).\end{aligned}\tag{2.1.4}$$

This governing equations are valid for the transmutation in the core at a given irradiation period. The origin of the time axis,  $\hat{t}$ , is set at the beginning of the irradiation period. The irradiation stops at time  $\hat{T}$ , and the fraction  $f$  of the fuel is to be discharged. The initial conditions for (2.1.4) are written as

$$\hat{C}_1(0) = \hat{C}_1^\circ, \quad \hat{C}_2(0) = \hat{C}_2^\circ, \quad \hat{C}_p(0) = \hat{C}_p^\circ.\tag{2.1.5}$$

$\hat{C}_j^\circ, j=1, 2$ , and  $p$ , are determined by considering the processes at the partitioning and the fuel fabrication, as shown in Section 2.1.3.

Notice that the sum of the right sides of three equations in (2.1.4) vanishes. This means that the quantity,  $\hat{C}_1(\hat{t}) + \hat{C}_2(\hat{t}) + \hat{C}_p(\hat{t})$ , is constant for  $0 \leq \hat{t} \leq \hat{T}$ . By the initial conditions (2.1.5),

$$\hat{C}_1(\hat{t}) + \hat{C}_2(\hat{t}) + \hat{C}_p(\hat{t}) = \hat{C}_1^\circ + \hat{C}_2^\circ + \hat{C}_p^\circ, \quad 0 \leq \hat{t} \leq \hat{T}.\tag{2.1.6}$$

We denote the quantity represented by the right side of (2.1.6) as a positive constant  $\hat{C}$ , *i.e.*,

$$\hat{C} \equiv \hat{C}_1^\circ + \hat{C}_2^\circ + \hat{C}_p^\circ.\tag{2.1.7}$$

By introducing the following non-dimensionalization,

$$\begin{aligned}C_1(t) &\equiv \frac{\hat{C}_1(\hat{t})}{\hat{C}}, \quad C_2(t) \equiv \frac{\hat{C}_2(\hat{t})}{\hat{C}}, \quad C_p(t) \equiv \frac{\hat{C}_p(\hat{t})}{\hat{C}}, \quad C_1^\circ \equiv \frac{\hat{C}_1^\circ}{\hat{C}}, \quad C_2^\circ \equiv \frac{\hat{C}_2^\circ}{\hat{C}}, \quad C_p^\circ \equiv \frac{\hat{C}_p^\circ}{\hat{C}}, \\ t &\equiv \frac{\hat{t}}{\hat{T}}, \quad d_1 \equiv \hat{d}_1\hat{T}, \quad d_2 \equiv \hat{d}_2\hat{T}, \quad p_2 \equiv \hat{p}_2\hat{T},\end{aligned}\tag{2.1.8}$$

the governing equations (2.1.4), the initial conditions (2.1.5), and the relationship (2.1.6) can be rewritten as

$$\begin{aligned}\frac{dC_1(t)}{dt} &= -d_1C_1(t), \\ \frac{dC_2(t)}{dt} &= -d_2C_2(t) + p_2C_1(t), \quad 0 < t < 1, \quad d_1 \geq p_2, \\ \frac{dC_p(t)}{dt} &= (d_1 - p_2)C_1(t) + d_2C_2(t),\end{aligned}\tag{2.1.9}$$

$$C_1(0) = C_1^\circ, \quad C_2(0) = C_2^\circ, \quad C_p(0) = C_p^\circ,\tag{2.1.10}$$

$$C_1(t) + C_2(t) + C_p(t) = C_1^\circ + C_2^\circ + C_p^\circ = 1, \quad 0 \leq t \leq 1.\tag{2.1.11}$$

The solutions for (2.1.9) subject to the initial conditions (2.1.10) are written as

---

<sup>4</sup>  $\hat{C}_p(\hat{t})$  is related to the number of atoms of all products generated by transmutation reactions in the two TRU radionuclides. However, because more than one atom could be generated by fission,  $\hat{C}_p(\hat{t})$  is *not* exactly same as the number of atoms of transmutation products. In this report, a pair of fission products is counted as a fictitious nuclide, and so  $\hat{C}_p(\hat{t})$  is equal to the number of atoms of all transmutation products. Hence,  $\hat{C}_p(\hat{t})$  is also called “the number of atoms of all transmutation products” in this report.

$$\begin{aligned}
C_1(t) &= C_1^{\circ} e^{-d_1 t}, \\
C_2(t) &= \begin{cases} C_2^{\circ} e^{-d_2 t} + \frac{P_2 C_1^{\circ}}{d_2 - d_1} (e^{-d_1 t} - e^{-d_2 t}), & d_1 \neq d_2, \\ (C_2^{\circ} + p_2 C_1^{\circ} t) e^{-d_2 t}, & d_1 = d_2, \end{cases} \\
C_p(t) &= \begin{cases} \frac{d_1 - d_2 - p_2}{d_1 - d_2} C_1^{\circ} (1 - e^{-d_1 t}) + \left( C_2^{\circ} + \frac{P_2}{d_1 - d_2} C_1^{\circ} \right) (1 - e^{-d_2 t}) + C_p^{\circ}, & d_1 \neq d_2, \\ (C_1^{\circ} + C_2^{\circ}) (1 - e^{-d_1 t}) - p_2 C_1^{\circ} t e^{-d_1 t} + C_p^{\circ}, & d_1 = d_2, \end{cases} \\
&0 \leq t \leq 1.
\end{aligned} \tag{2.1.12}$$

Notice that the sum,  $C_1(t) + C_2(t) + C_p(t)$ , actually becomes  $C_1^{\circ} + C_2^{\circ} + C_p^{\circ}$ , which is unity, as shown by (2.1.11).

We are primarily interested in the values at the end of the irradiation period. These are obtained by substituting  $t=1$  into the above equations, resulting in

$$\begin{aligned}
C_1(1) &= C_1^{\circ} e^{-d_1}, \\
C_2(1) &= \begin{cases} C_2^{\circ} e^{-d_2} + \frac{P_2 C_1^{\circ}}{d_2 - d_1} (e^{-d_1} - e^{-d_2}), & d_1 \neq d_2, \\ (C_2^{\circ} + p_2 C_1^{\circ} T) e^{-d_2 T}, & d_1 = d_2, \end{cases} \\
C_p(1) &= \begin{cases} \frac{d_1 - d_2 - p_2}{d_1 - d_2} C_1^{\circ} (1 - e^{-d_1}) + \left( C_2^{\circ} + \frac{P_2}{d_1 - d_2} C_1^{\circ} \right) (1 - e^{-d_2}) + C_p^{\circ}, & d_1 \neq d_2, \\ (C_1^{\circ} + C_2^{\circ}) (1 - e^{-d_1}) - p_2 C_1^{\circ} e^{-d_1} + C_p^{\circ}, & d_1 = d_2. \end{cases}
\end{aligned} \tag{2.1.13}$$

Solutions (2.1.13) can be written in the vector and matrix notations, which simplify the further mathematical derivation, as

$$\underline{C} = \underline{A} \underline{C}^{\circ}, \tag{2.1.14}$$

where

$$\underline{C} \equiv \begin{bmatrix} C_1(1) \\ C_2(1) \end{bmatrix}, \underline{C}^{\circ} \equiv \begin{bmatrix} C_1^{\circ} \\ C_2^{\circ} \end{bmatrix}, \tag{2.1.15}$$

and

$$\underline{A} \equiv \begin{bmatrix} a_{11} & 0 \\ a_{21} & a_{22} \end{bmatrix}, \text{ where } \begin{cases} a_{11} = e^{-d_1}, \\ a_{21} = \begin{cases} \frac{P_2}{d_2 - d_1} (e^{-d_1} - e^{-d_2}), & d_1 \neq d_2, \\ p_2 e^{-d_2}, & d_1 = d_2, \end{cases} \\ a_{22} = e^{-d_2}. \end{cases} \tag{2.1.16}$$

The transmutation matrix  $\underline{A}$  is constant because the parameters in this matrix are assumed to be constant. Equations (2.1.14), (2.1.15), and (2.1.16) show that the numbers of atoms of radionuclides after transmutation can be obtained as the product of the starting numbers for a given cycle by the transmutation matrix  $\underline{A}$ .

### 2.1.3 Treatment of Irradiated ATW Fuel

**Discharge:** After the irradiation period,  $\hat{T}$  [yr], a fraction<sup>5</sup>  $f$  of the fuel in the core is discharged for partitioning and make-up. The fraction  $(1 - f)$  of the fuel remains in the core.

The fraction  $fC_j(1)$  of radionuclide  $j$ ,  $j=1, 2, p$ , is included in the discharged fuel, whereas the fraction  $(1 - f)C_j(1)$  of radionuclide  $j$  remains in the core.

**Partitioning:** The discharged fuel goes to the partitioning process, where the transmutation products

<sup>5</sup> The fraction  $f$  is defined as the ratio of the number of atoms included in the discharged fuel to the number of atoms included in the core at the end of irradiation. Due to fissions, one atom can be split into two or more atoms. We count those atoms resulting from fission as one atom. See also the footnote 4.



are chemically separated from TRU radionuclides. It is assumed that a fraction<sup>6</sup>  $\alpha$  of TRU radionuclides, 1 or 2, in the discharged fuel is *not* recovered by the partitioning process, but is included in the waste. It is assumed that the identical value of  $\alpha$  is applied for both TRU radionuclides. The fraction  $(1-\alpha)$  of TRU is recovered by the partitioning, and re-used as fuel material in the fabrication stage.

The fraction of radionuclide  $j$  that is included in the waste,  $L_j$ , is given by

$$\begin{aligned} L_j &= \alpha f C_j(1), \quad j=1,2, \\ L_p &= f C_p(1). \end{aligned} \quad (2.1.17)$$

The fraction,  $X_j$ ,  $j = 1, 2$ , and  $p$ , of radionuclide  $j$  in the discharged fuel that is recovered at the partitioning and utilized for fuel fabrication is given by

$$\begin{aligned} X_j &= (1-\alpha) f C_j(1), \quad j=1,2, \\ X_p &= 0. \end{aligned} \quad (2.1.18)$$

Notice that the sum of  $L_j$  and  $X_j$  is equal to the fraction,  $f C_j(1)$ , for radionuclide  $j$  in the discharged fuel. At the partitioning, the following balance equation holds:

$$(L_1 + L_2 + L_p) + (X_1 + X_2) = f. \quad (2.1.19)$$

**Fabrication:** The fuel is prepared for the next irradiation period by adding the two TRU radionuclides from the storage, because the sum of the numbers of atoms of the two radionuclides recovered by the partitioning is smaller than the number,  $f \hat{C}$ , of atoms included in the discharged fuel. The difference between before and after the partitioning, or the *deficit*, is filled with the mixture of the two TRU radionuclides in the storage. It is assumed that the fractions,  $\gamma_1$  and  $\gamma_2$ , are kept, *i.e.*, neither nuclide will be preferentially utilized for the fuel make-up.

We define the deficit  $\Delta$  as

$$\Delta \equiv L_1 + L_2 + L_p. \quad (2.1.20)$$

By (2.1.19),

$$\Delta = f - (X_1 + X_2). \quad (2.1.21)$$

The deficit is assumed to be made up by the material from the TRU storage. The material in the storage contains two TRU radionuclides with the compositions of  $\gamma_1$  and  $\gamma_2$ . Therefore, for radionuclide 1, the fraction,  $X_1$ , coming from the partitioning, and the fraction,  $\gamma_1 \Delta$ , are included in the fabricated fuel. Similarly, for radionuclide 2,  $X_2$  and  $\gamma_2 \Delta$  are included<sup>7</sup>.

**Installation:** This returning fuel fulfils the fraction  $f$  of the transmuter core, and is uniformized with the remaining fraction  $(1-f)C_j(1)$ ,  $j = 1, 2, p$ , in the core. Thus, the fractions of the two TRU radionuclides and transmutation products at the beginning of the next cycle are determined. It is assumed that the partitioning and fuel fabrication are made instantaneously. The following irradiation period starts immediately after the end of the preceding irradiation period.

The fractions  $C_j^{\circ'}$ ,  $j = 1, 2$ , of TRU radionuclides and that  $C_p^{\circ'}$  of transmutation products in the core after adding the fabricated fuel and before the beginning of the next irradiation period are formulated as

$$\begin{aligned} C_j^{\circ'} &= \gamma_j \Delta + X_j + (1-f) C_j(1), \quad j=1,2, \\ C_p^{\circ'} &= (1-f) C_p(1). \end{aligned} \quad (2.1.22)$$

Equation (2.1.22) for  $j=1$  and 2 can be expressed in a matrix form.

$$\underline{C}^{\circ'} = \underline{B} \underline{C} + f \underline{\gamma}, \quad (2.1.23)$$

where

$$\underline{C}^{\circ'} \equiv \begin{bmatrix} C_1^{\circ'} \\ C_2^{\circ'} \end{bmatrix}, \quad \underline{\gamma} \equiv \begin{bmatrix} \gamma_1 \\ \gamma_2 \end{bmatrix}, \quad \text{and} \quad (2.1.24)$$

$$\underline{B} \equiv \begin{bmatrix} 1-\alpha f - (1-\alpha)\gamma_1 f & -(1-\alpha)\gamma_1 f \\ -(1-\alpha)\gamma_2 f & 1-\alpha f - (1-\alpha)\gamma_2 f \end{bmatrix}. \quad (2.1.25)$$

<sup>6</sup> The fraction  $\alpha$  is defined as the ratio of the number of atoms of TRU radionuclides that are *not* recovered by partitioning to the number of atoms of TRU radionuclides that are included in the discharged fuel.

<sup>7</sup> It can be readily shown that the sum of  $X_1$ ,  $X_2$ ,  $\gamma_1 \Delta$ , and  $\gamma_2 \Delta$  becomes  $f$  by (2.1.1) and (2.1.21).

The matrix  $\underline{B}$  represents the characteristics of the partitioning, the fuel fabrication, and the uniformization of the fuel in the core. In this report, this matrix is called the partitioning matrix.

With (2.1.14) and (2.1.23),

$$\underline{C}^{\circ'} = \underline{B}\underline{A}\underline{C}^{\circ} + f\underline{\gamma} . \quad (2.1.26)$$

Equation (2.1.26) shows that the fractions of TRU radionuclides in a chain after the irradiation and the partitioning are determined by two matrices  $\underline{B}$  and  $\underline{A}$ , and that the two vectors,  $\underline{C}^{\circ'}$  and  $\underline{C}^{\circ}$ , are related. The vector  $\underline{C}^{\circ}$  represents the fractions of radionuclides in the core before the irradiation of the present cycle, while the vector  $\underline{C}^{\circ'}$  represents the fractions of radionuclides in the core after partitioning, fuel fabrication, and uniformization of the core. The vector  $\underline{C}^{\circ'}$  is considered to be the initial conditions for the following cycle. Thus, we can formulate the change of radionuclide fractions in the core as a function of the cycle number,  $i$ .

The processes from the second irradiation and on are the same as those described above. A “cycle” is defined as a series of events that occur in the time period between the beginning of irradiation in the transmuter and the installation of the made-up fuel into the transmuter core for next irradiation. The fuel resides in the core for the time period,  $\hat{T}$  [yr]. For simplicity, we assume that the irradiation period,  $\hat{T}$ , is identical for all cycles.<sup>8</sup>

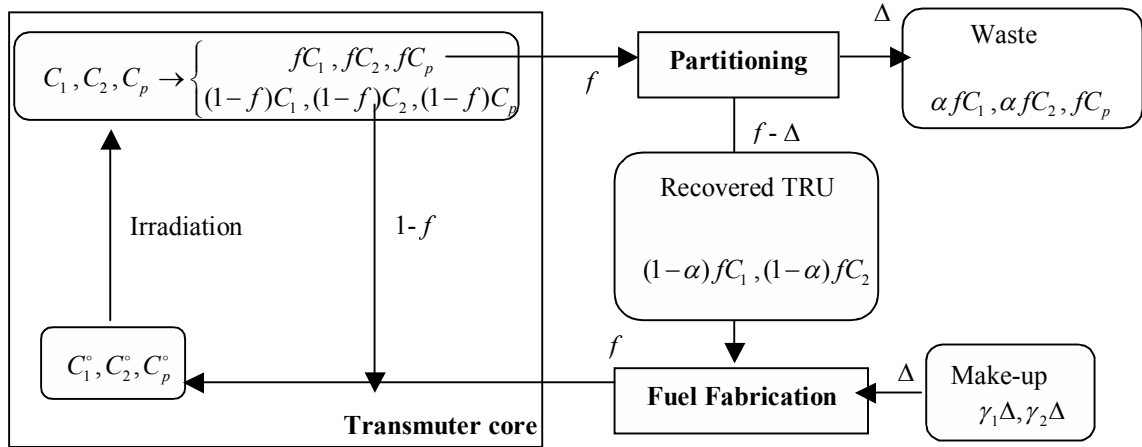


**Figure 2-1:** Schematical diagram for mass flow in the simplified system. Square boxes represent processes, while the boxes with rounded corners represent materials that are derived from or fed into a process. See Eqs. (2.1.1), (2.1.8) and (2.1.20) for the definitions for non-dimensionalized quantities.

#### 2.1.4 Ranges of System Parameters

In the present model, there are seven parameters that determine the system behavior. These are the irradiation time period,  $\hat{T}$ , the production coefficient,  $\hat{p}_2$ , of the second member, the destruction coefficients,  $\hat{d}_1$  and  $\hat{d}_2$ , of the first and second members, the waste fraction,  $\alpha$ , the core fraction,  $f$ , discharged at the end of irradiation, and the fractions,  $\gamma_1$  and  $\gamma_2$ , of the first and second members in the TRU storage. Notice that  $\gamma_1$  and  $\gamma_2$  are related by (2.1.1). We call these the *system parameters* hereafter. It is assumed that the system parameters are constant with time and the number of cycles.

There are some constraints on the system parameters from physical considerations.

First,  $\hat{T} \geq 0$ . The case with  $\hat{T} = 0$  represents no transmutation. All the TRU radionuclides originally

<sup>8</sup> The irradiation time should be determined by checking the reactivity of the fuel or the neutron multiplication factor of the core. In reality, the irradiation time can be different from one cycle to another.

included in the LWR spent fuel with compositions  $\gamma_1$  and  $\gamma_2$  will eventually become waste.

The production and destruction coefficients,  $\hat{p}_2, \hat{d}_1 \geq 0$ . Also, the condition (2.1.3) should be satisfied. The destruction coefficient should satisfy  $\hat{d}_2 \geq 0$ .

The fraction  $\alpha$  ranges in  $0 < \alpha \leq 1$ . The case with  $\alpha = 1$  corresponds to no partitioning, hence no recycling. All the discharged fuel is regarded as waste<sup>9</sup>. The case with  $\alpha = 0$  means perfect recovery of TRU radionuclides, which is impossible thermodynamically. Thus, this case is excluded.

The core fraction discharged,  $f$ , ranges in  $0 < f \leq 1$ . The case with  $f = 0$  is excluded, because no irradiated fuel could come out of the transmuted. For the case with  $f = 1$ , all the fuel in the core is discharged at the end of an irradiation period. If  $f = 1$  and  $\alpha = 1$ , the situation is similar to the case, where a reactor is used only for one irradiation period with initially loaded fuel, and then the whole spent fuel is disposed of after the irradiation period [4].

The losses of TRU radionuclides from the recycling at the fuel fabrication are not included in the present model, and should be incorporated in future extension.

## 2.2 Analytical Solutions for Multiple Cycles

### 2.2.1 Recursive Solutions for Multiple Cycles

For multiple cycles, the aforementioned formulations, (2.1.14) and (2.1.26), are utilized as that for the  $i$ -th cycle in general, and rewritten as

$$\underline{C}^{(i)} = \underline{\underline{A}}\underline{C}^{s(i-1)}, \quad i=1, 2, \dots, \quad (2.2.1)$$

$$\underline{C}^{s(i)} = \underline{\underline{B}}\underline{C}^{(i)} + f\underline{\gamma}, \quad i=1, 2, \dots, \quad (2.2.2)$$

where

$$\underline{C}^{(i)} \equiv \begin{bmatrix} C_1^{(i)} \\ C_2^{(i)} \end{bmatrix}, \underline{C}^{s(i)} \equiv \begin{bmatrix} C_1^{s(i)} \\ C_2^{s(i)} \end{bmatrix}, \underline{\gamma} \equiv \begin{bmatrix} \gamma_1 \\ \gamma_2 \end{bmatrix}. \quad (2.2.3)$$

For the first cycle ( $i = 1$ ), Equation (2.2.1) reads

$$\underline{C}^{(1)} = \underline{\underline{A}}\underline{C}^{s(0)}. \quad (2.2.4)$$

The vector  $\underline{C}^{s(0)}$  represents the fractions of radionuclides in the core at the beginning of the irradiation of the first cycle. This fuel is assumed to be prepared by the material from the TRU storage, and to have the same compositions as  $\gamma_1$  and  $\gamma_2$ . No transmutation products are included in the fuel. Hence, the vector  $\underline{C}^{s(0)}$  is given by

$$\underline{C}^{s(0)} = \underline{\gamma} = \begin{bmatrix} \gamma_1 \\ \gamma_2 \end{bmatrix}. \quad (2.2.5)$$

Also, it is assumed that

$$C_p^{s(0)} = 0. \quad (2.2.6)$$

With (2.2.5), the fractions of two radionuclides after the irradiation in the first cycle are obtained by (2.2.4). The fractions at the beginning of the second cycle are obtained by setting  $i=1$  in (2.2.2). In this fashion, we can calculate the fractions of two TRU radionuclides at the beginning and at the end of irradiation periods recursively for multiple cycles.

A drawback of using the recursive solutions for numerical calculations is that we need to calculate all the values of  $\underline{C}^{(i)}$  and  $\underline{C}^{s(i)}$  at the preceding cycles to obtain the values of those vectors at the present cycle. Effects of the system parameters on the various quantities of interest, such as  $\underline{C}^{(i)}$ , are not explicitly observed by the recursive solutions.

### 2.2.2 Non-Recursive Solutions for Multiple Cycles

Non-recursive solutions are obtained in this section, based on the recursive solutions (2.2.1), (2.2.2), and (2.2.3). First, we derive the solutions for the first, second, and third cycles for illustration.

The first cycle ( $i=1$ ):

<sup>9</sup> This situation is often called “direct disposal.”

The fractions of radionuclides at the beginning of the first cycle are prescribed by (2.2.5) and (2.2.6). The fractions of TRU radionuclides after the irradiation period are given by (2.2.4). With these known, the fraction  $C_p^{(1)}$  of transmutation products is calculated by  $1 - C_1^{(1)} - C_2^{(1)}$  (see (2.1.11)). By the partitioning, fuel fabrication, and core uniformization, the fractions of radionuclides in the core are obtained by (2.2.2) as

$$\underline{C}^{(1)} = \underline{B}\underline{C}^{(1)} + f\underline{\gamma}. \quad (2.2.7)$$

By substituting (2.2.4) and (2.2.5),

$$\underline{C}^{(1)} = \left( \underline{R} + f\underline{I} \right) \underline{\gamma}. \quad (2.2.8)$$

Here, we define the system matrix  $\underline{R}$  as

$$\underline{R} \equiv \underline{B}\underline{A} = \begin{bmatrix} r_{11} & r_{12} \\ r_{21} & r_{22} \end{bmatrix}, \quad (2.2.9)$$

where

$$\begin{aligned} r_{11} &= [1 - \alpha f - (1 - \alpha)\gamma_1 f] e^{-d_1} - (1 - \alpha)\gamma_1 f a_{21}, \\ r_{12} &= -(1 - \alpha)\gamma_1 f e^{-d_2}, \\ r_{21} &= -(1 - \alpha)\gamma_2 f e^{-d_1} + [1 - \alpha f - (1 - \alpha)\gamma_2 f] a_{21}, \\ r_{22} &= [1 - \alpha f - (1 - \alpha)\gamma_2 f] e^{-d_2}. \end{aligned} \quad (2.2.10)$$

The second cycle ( $i=2$ ):

By (2.2.1),

$$\underline{C}^{(2)} = \underline{A}\underline{C}^{(1)} \quad (2.2.11)$$

Substituting (2.2.8) into (2.2.11) yields

$$\underline{C}^{(2)} = \underline{A} \left( \underline{R} + f\underline{I} \right) \underline{\gamma}. \quad (2.2.12)$$

By substituting (2.2.12) into (2.2.2),

$$\underline{C}^{(2)} = \underline{B}\underline{A} \left( \underline{R} + f\underline{I} \right) \underline{\gamma} + f\underline{\gamma}.$$

By (2.2.9), this simplifies as

$$\underline{C}^{(2)} = \left( \underline{R}^2 + f\underline{R} + f\underline{I} \right) \underline{\gamma}. \quad (2.2.13)$$

The third cycle ( $i=3$ )

Similarly, we can obtain two expressions:

$$\underline{C}^{(3)} = \underline{A} \left( \underline{R}^2 + f\underline{R} + f\underline{I} \right) \underline{\gamma}, \quad (2.2.14)$$

and

$$\underline{C}^{(3)} = \left( \underline{R}^3 + f\underline{R}^2 + f\underline{R} + f\underline{I} \right) \underline{\gamma}. \quad (2.2.15)$$

General expressions for the  $k$ -th cycle are given as

$$\underline{C}^{(1)} = \underline{A} \underline{\gamma}, \quad \underline{C}^{(1)} = \left( \underline{R} + f\underline{I} \right) \underline{\gamma}, \quad (2.2.16)$$

$$\underline{C}^{(k+2)} = \underline{A} \left( \underline{R}^{k+1} + f \sum_{j=0}^k \underline{R}^j \right) \underline{\gamma}, \quad \underline{C}^{(k+2)} = \left( \underline{R}^{k+2} + f \sum_{j=0}^{k+1} \underline{R}^j \right) \underline{\gamma}, \quad k = 0, 1, 2, \dots \quad (2.2.17)$$

The general non-recursive solutions (2.2.16) and (2.2.17) include the multiplication of  $\underline{R}$ , and were introduced and developed by one of the authors [5]. To explicitly display the system parameters, the similarity transformation is introduced. Let  $\underline{R}$  be an  $n \times n$  matrix. Then  $\lambda$  is an eigenvalue of  $\underline{R}$  if and only if

$$p(\lambda) = \det(\underline{R} - \lambda \underline{I}) = 0. \quad (2.2.18)$$

This is called the characteristic equation of the system matrix  $\underline{R}$ ;  $p(\lambda)$  is called the characteristic polynomial of  $\underline{R}$ . This is a polynomial of degree  $n$ . By the fundamental theorem of algebra, any polynomial of degree  $n$  with real or complex coefficients has exactly  $n$  roots counting multiplicity. The eigenvalues are roots of the characteristic equation,

$$p(\lambda) = \begin{vmatrix} r_{11} - \lambda & r_{12} \\ r_{21} & r_{22} - \lambda \end{vmatrix} = \lambda^2 - (r_{11} + r_{22})\lambda + r_{11}r_{22} - r_{12}r_{21} = 0. \quad (2.2.19)$$

The roots of the above characteristic equation are the eigenvalues of the system matrix  $\underline{R}$ . Solving the quadratic equation, we get the eigenvalues  $\lambda_1$  and  $\lambda_2$  such as

$$\lambda_{1,2} = \frac{1}{2} \left[ r_{11} + r_{22} \pm \sqrt{(r_{11} + r_{22})^2 - 4(r_{11}r_{22} - r_{12}r_{21})} \right]. \quad (2.2.20)$$

The sum of the diagonal elements of the matrix  $\underline{R}$  is called the trace and is denoted as  $\text{tr}(\underline{R})$ . By (2.2.20), the trace is equal to the sum of two eigenvalues, *i.e.*,

$$\text{tr}(\underline{R}) = r_{11} + r_{22} = \lambda_1 + \lambda_2. \quad (2.2.21)$$

Also, the multiplication of the two eigenvalues is equal to the determinant of the matrix, given by

$$\det(\underline{R}) = r_{11}r_{22} - r_{12}r_{21} = \lambda_1\lambda_2. \quad (2.2.22)$$

Therefore, the characteristic polynomial is expressed as

$$\lambda^2 - \text{tr}(\underline{R})\lambda + \det(\underline{R}) = 0. \quad (2.2.23)$$

By substituting (2.2.10), the trace and the determinant of the system matrix  $\underline{R}$  can be written as

$$\text{tr}(\underline{R}) = (1 - \alpha f)\exp(-d_1) + (1 - f)\exp(-d_2) + \gamma_1 f(1 - \alpha) [\exp(-d_2) - \exp(-d_1) - a_{21}], \quad (2.2.24)$$

$$\det(\underline{R}) = (1 - f)(1 - \alpha f)\exp(-d_1)\exp(-d_2). \quad (2.2.25)$$

As shown in (2.2.24) and (2.2.25), the eigenvalues are determined by the values of the system parameters. The system parameters take the following ranges:

$$0 < \alpha \leq 1, \quad 0 < f \leq 1, \quad d_1 \geq 0, \quad d_2 \geq 0, \quad d_1 \geq p_2 \geq 0, \quad 0 < \gamma_1 \leq 1, \quad 0 \leq \gamma_2 < 1, \quad (2.2.26)$$

$$\gamma_1 + \gamma_2 = 1$$

We consider the similarity transformation for Case (I)  $0 < \alpha < 1$  and Case (II)  $\alpha = 1$ . Case (I) corresponds to the recycling case, where the partitioning is made. Case (II) corresponds to the once-through cycle, where no partitioning is made and all the discharged fuel from the transmuter is destined to a repository directly. For each of these two cases, we consider the case for  $\lambda_1 \neq \lambda_2$  and the case for  $\lambda_1 = \lambda_2$ . For the former case, the two eigenvalues are distinct. For the latter case, there is only one distinct eigenvalue with multiplicity equal to 2.

In any of the aforementioned cases, eigenvalues cannot be equal to 1 for the system parameter ranges shown in (2.2.26). The proof is shown in Appendix for this chapter.

In the following subsections, the similarity transformations for Cases (I) and (II) are developed, and general non-recursive solutions for the fractions of two radionuclides in the transmuter core as a function of the cycle number,  $i$ .

**(a) Case (I): Recycling Case ( $0 < \alpha < 1$ )**

In this case, the element  $r_{12}$  of the system matrix is smaller than 0 (*not* equal to zero), *i.e.*,

$$r_{12} = -(1 - \alpha)\gamma_1 f \exp(-d_1) < 0. \quad (2.2.27)$$

We consider the case for  $\lambda_1 \neq \lambda_2$  and the case for  $\lambda_1 = \lambda_2$ .

**(a.1)  $\lambda_1 \neq \lambda_2$**

Let  $\underline{X}$  be an  $n \times n$  matrix whose column vectors  $\underline{x}_1, \dots, \underline{x}_n$  are eigenvectors of  $\underline{R}$  corresponding to the eigenvalues  $\lambda_1, \dots, \lambda_n$  of  $\underline{R}$ . If  $\underline{x}_1, \dots, \underline{x}_n$  are linearly independent, then

$$\underline{X}^{-1} \underline{R} \underline{X} = \underline{D} \quad \text{or} \quad \underline{R} = \underline{X} \underline{D} \underline{X}^{-1}. \quad (2.2.28)$$

where  $\underline{D}$  is the diagonal matrix with elements  $\lambda_1, \dots, \lambda_n$  in the principal diagonal. Eigenvectors corresponding to distinct eigenvalues are also linearly independent. Thus,  $\underline{R}$  and  $\underline{D}$  are similar in that  $\underline{R}$  and  $\underline{D}$  have the same eigenvalues. Its eigenvalue matrix  $\underline{D}$  and eigenvector matrix  $\underline{X}$  describe the system matrix  $\underline{R}$ . The system matrix  $\underline{R}$  is replaced with these matrices  $\underline{D}$  and  $\underline{X}$ , and then we get the non-recursive form equations with these matrices.

The multiplication of the system matrix can be reduced to the multiplication of the eigenvalue matrix; the eigenvalue matrix has the diagonal elements only. Let us simplify the expression for the fractions after transmutation and refueling using the similarity transformation. The square of the system matrix  $\underline{R}$  can be written as

$$\underline{R}^2 = (\underline{X} \underline{D} \underline{X}^{-1}) (\underline{X} \underline{D} \underline{X}^{-1}) = \underline{X} \underline{D} (\underline{X}^{-1} \underline{X}) \underline{D} \underline{X}^{-1} = \underline{X} \underline{D} \underline{I} \underline{D} \underline{X}^{-1} = \underline{X} \underline{D}^2 \underline{X}^{-1}. \quad (2.2.29)$$

This can be generalized for the  $i$ -th power of the system matrix  $\underline{R}$  and it is written as

$$\underline{R}^i = \underline{X} \underline{D}^i \underline{X}^{-1}. \quad (2.2.30)$$

When we insert this expression into the expressions (2.2.17), they are expressed in terms of the

eigenvalue matrix and the eigenvector matrix as

$$\underline{C}^{(k+2)} = \underline{A}X \left( \underline{D}^{k+1} + f \sum_{j=0}^k \underline{D}^j \right) X^{-1} \underline{\gamma}, \quad \underline{C}^{(k+2)} = X \left( \underline{D}^{k+2} + f \sum_{j=0}^{k+1} \underline{D}^j \right) X^{-1} \underline{\gamma}, \quad k = 0, 1, 2, \dots, \quad \underline{D}^0 = I. \quad (2.2.31)$$

At this point, the matrix multiplication itself becomes much simpler than the previous one (2.2.17) although the equation looks like similar before and after similarity transformation. The eigenvalue matrix  $\underline{D}$  has its diagonal elements only. Thus, the multiple power of this matrix and the summation of this multiple power of matrix can be done by simple manipulation. Let us first consider the multiple power of eigenvalue matrix  $\underline{D}$ . It can be written as

$$\underline{D}^{k+1} = \overbrace{\begin{bmatrix} \lambda_1 & 0 \\ 0 & \lambda_2 \end{bmatrix}}^{k+1} \dots \overbrace{\begin{bmatrix} \lambda_1 & 0 \\ 0 & \lambda_2 \end{bmatrix}}^{k+1} = \begin{bmatrix} \lambda_1^{k+1} & 0 \\ 0 & \lambda_2^{k+1} \end{bmatrix}. \quad (2.2.32)$$

Also the finite sum of the multiple power of  $\underline{D}$  can be written as

$$\sum_{m=0}^k \underline{D}^m = \begin{bmatrix} 1 & 0 \\ 0 & 1 \end{bmatrix} + \begin{bmatrix} \lambda_1 & 0 \\ 0 & \lambda_2 \end{bmatrix} + \dots + \begin{bmatrix} \lambda_1^k & 0 \\ 0 & \lambda_2^k \end{bmatrix} = \begin{bmatrix} \sum_{m=0}^k \lambda_1^m & 0 \\ 0 & \sum_{m=0}^k \lambda_2^m \end{bmatrix}, \quad (2.2.33)$$

where the summation in this expression can be simplified further, noticing that eigenvalues are not equal to 1, using the geometric series such as

$$\sum_{m=0}^k \lambda_1^m = \frac{1 - \lambda_1^{k+1}}{1 - \lambda_1}, \quad \sum_{m=0}^k \lambda_2^m = \frac{1 - \lambda_2^{k+1}}{1 - \lambda_2}. \quad (2.2.34)$$

The eigenvectors corresponding to the eigenvalues can be obtained by solving the following homogeneous system

$$(\underline{R} - \lambda_\ell I) \underline{x} = \underline{0}, \quad \ell = 1, 2, \quad (2.2.35)$$

or

$$\begin{bmatrix} r_{11} - \lambda_\ell & r_{12} \\ r_{21} & r_{22} - \lambda_\ell \end{bmatrix} \begin{bmatrix} x_1 \\ x_2 \end{bmatrix} = \begin{bmatrix} 0 \\ 0 \end{bmatrix}, \quad \ell = 1, 2. \quad (2.2.36)$$

The eigenvectors for  $\ell = 1$  and 2 can be obtained from (2.2.36) such as

$$\underline{x}_1 = \begin{bmatrix} r_{12} \\ \lambda_1 - r_{11} \end{bmatrix}, \quad \underline{x}_2 = \begin{bmatrix} r_{12} \\ \lambda_2 - r_{11} \end{bmatrix}. \quad (2.2.37)$$

Then, the eigenvector matrix can be written such as

$$\underline{X} = \begin{bmatrix} r_{12} & r_{12} \\ \lambda_1 - r_{11} & \lambda_2 - r_{11} \end{bmatrix}. \quad (2.2.38)$$

Noticing that, in case (I),  $r_{12} \neq 0$ , the inverse matrix of the eigenvector matrix can be written as

$$\underline{X}^{-1} = \frac{1}{r_{12}(\lambda_2 - \lambda_1)} \begin{bmatrix} \lambda_2 - r_{11} & -r_{12} \\ -(\lambda_1 - r_{11}) & r_{12} \end{bmatrix}, \quad \lambda_1 \neq \lambda_2. \quad (2.2.39)$$

Let us apply all these manipulation to (2.2.31), resulting in the non-recursive solutions,

$$\begin{bmatrix} C_1^{(i)} \\ C_2^{(i)} \end{bmatrix} = \underline{A}X \begin{bmatrix} \lambda_1^{i-1} + \frac{f(1 - \lambda_1^{i-1})}{1 - \lambda_1} & 0 \\ 0 & \lambda_2^{i-1} + \frac{f(1 - \lambda_2^{i-1})}{1 - \lambda_2} \end{bmatrix} X^{-1} \underline{\gamma}, \quad i = 1, 2, 3, \dots, \quad \lambda_1 \neq \lambda_2, \quad 0 < \alpha < 1, \quad (2.2.40)$$

$$\begin{bmatrix} C_1^{(i)} \\ C_2^{(i)} \end{bmatrix} = X \begin{bmatrix} \lambda_1^i + \frac{f(1 - \lambda_1^i)}{1 - \lambda_1} & 0 \\ 0 & \lambda_2^i + \frac{f(1 - \lambda_2^i)}{1 - \lambda_2} \end{bmatrix} X^{-1} \underline{\gamma}, \quad i = 0, 1, 2, 3, \dots, \quad \lambda_1 \neq \lambda_2, \quad 0 < \alpha < 1. \quad (2.2.41)$$

**(a.2)**  $\lambda_1 = \lambda_2 = \lambda$

We assume that the only distinct eigenvalue is equal to  $\lambda$ . For this case, we can also determine two

eigenvectors, with which the eigenvector matrix  $\underline{X}$  can be written as follows:

$$\underline{X} = \begin{bmatrix} r_{12} & r_{12} \\ \lambda - r_{11} & 1 + \lambda - r_{11} \end{bmatrix}, \quad \underline{X}^{-1} = \frac{1}{r_{12}} \begin{bmatrix} 1 + \lambda - r_{11} & -r_{12} \\ -\lambda + r_{11} & r_{12} \end{bmatrix}. \quad (2.2.42)$$

Then,

$$\underline{X}^{-1} \underline{R} \underline{X} = \begin{bmatrix} \lambda & 1 \\ 0 & \lambda \end{bmatrix}. \quad (2.2.43)$$

If the upper triangular matrix on the right hand side is denoted as  $\underline{D}$  for this case, then

$$\underline{R} = \underline{X} \underline{D} \underline{X}^{-1} \text{ and } \underline{R}^i = \underline{X} \underline{D}^i \underline{X}^{-1}, \quad (2.2.44)$$

where

$$\underline{D}^{k+1} = \begin{bmatrix} \lambda & 1 \\ 0 & \lambda \end{bmatrix} \cdots \begin{bmatrix} \lambda & 1 \\ 0 & \lambda \end{bmatrix} = \begin{bmatrix} \lambda_1^{k+1} & (k+1)\lambda^k \\ 0 & \lambda_2^{k+1} \end{bmatrix} \quad (2.2.45)$$

Let us apply all these manipulation to (2.2.31), resulting in the non-recursive solutions,

$$\begin{bmatrix} C_1^{(i)} \\ C_2^{(i)} \end{bmatrix} = \underline{A} \underline{X} \begin{bmatrix} \lambda^{i-1} + \frac{f(1-\lambda^{i-1})}{1-\lambda} & (i-1)\lambda^{i-2} + f \left\{ \frac{1-\lambda^{i-2}}{(1-\lambda)^2} - \frac{(i-2)\lambda^{i-2}}{1-\lambda} \right\} \\ 0 & \lambda^{i-1} + \frac{f(1-\lambda^{i-1})}{1-\lambda} \end{bmatrix} \underline{X}^{-1} \underline{\gamma}, \quad (2.2.46)$$

$$i = 1, 2, 3, \dots, \lambda_1 = \lambda_2, \quad 0 < \alpha < 1,$$

$$\begin{bmatrix} C_1^{(i)} \\ C_2^{(i)} \end{bmatrix} = \underline{X} \begin{bmatrix} \lambda^i + \frac{f(1-\lambda^i)}{1-\lambda} & i\lambda^{i-1} + f \left\{ \frac{1-\lambda^{i-1}}{(1-\lambda)^2} - \frac{(i-1)\lambda^{i-1}}{1-\lambda} \right\} \\ 0 & \lambda^i + \frac{f(1-\lambda^i)}{1-\lambda} \end{bmatrix} \underline{X}^{-1} \underline{\gamma}, \quad (2.2.47)$$

$$i = 0, 1, 2, 3, \dots, \lambda_1 = \lambda_2, \quad 0 < \alpha < 1$$

**(b) Case (II): Once-Through Case ( $\alpha = 1$ )**

In this case, the element  $r_{12}$  is equal to zero. By (2.2.10),

$$r_{11} = (1-f)e^{-d_1}, \quad r_{12} = 0, \quad r_{21} = (1-f)a_{21}, \quad r_{22} = (1-f)e^{-d_2}. \quad (2.2.48)$$

From (2.2.24) and (2.2.25), the trace and the determinant are written as

$$\text{tr}(\underline{R}) = (1-f)\exp(-d_1) + (1-f)\exp(-d_2), \quad (2.2.49)$$

$$\det(\underline{R}) = (1-f)^2 \exp(-d_1)\exp(-d_2). \quad (2.2.50)$$

The eigenvalues can be obtained as

$$\lambda_1 = (1-f)\exp(-d_1), \quad \lambda_2 = (1-f)\exp(-d_2) \quad (2.2.51)$$

It is remarkable that for this case the eigenvalues are always smaller than 1 and greater than or equal to 0.

We consider the case for  $\lambda_1 \neq \lambda_2$  and the case for  $\lambda_1 = \lambda_2$ .

For the two eigenvalues to be distinct, it must be satisfied that

$$0 < f < 1 \text{ and } d_1 \neq d_2. \quad (2.2.52)$$

For only one distinct eigenvalue with multiplicity equal to 2, we have two cases: (i)  $0 < f < 1$  and  $d_1 = d_2$ , and (ii)  $f = 1$ .

We consider these three cases hereafter.

**(b.1)  $\lambda_1 \neq \lambda_2$  ( $0 < f < 1$  and  $d_1 \neq d_2$ )**

The eigenvector matrix and its inverse can be obtained as

$$\underline{X} = \begin{bmatrix} \exp(-d_1) - \exp(-d_2) & 0 \\ a_{21} & 1 \end{bmatrix}, \quad \underline{X}^{-1} = \frac{1}{\exp(-d_1) - \exp(-d_2)} \begin{bmatrix} 1 & 0 \\ -a_{21} & \exp(-d_1) - \exp(-d_2) \end{bmatrix}. \quad (2.2.53)$$

Then,

$$\underline{\underline{X}}^{-1} \underline{\underline{R}} \underline{\underline{X}} = \begin{bmatrix} \lambda_1 & 0 \\ 0 & \lambda_2 \end{bmatrix}. \quad (2.2.54)$$

The rest of the solution procedure is the same as that for the case (a.1) shown above. The non-recursive solutions (2.2.40) and (2.2.41) apply for this case.

**(b.2)**  $\lambda_1 = \lambda_2$  ( $0 < f < 1$  and  $d_1 = d_2 = d$ )

In this case, the eigenvalue is equal to  $\lambda = (1-f)\exp(-d)$ . The eigenvector matrix and its inverse can be obtained as

$$\underline{\underline{X}} = \begin{bmatrix} 0 & 1 \\ (1-f)a_{21} & 0 \end{bmatrix}, \quad \underline{\underline{X}}^{-1} = \begin{bmatrix} 0 & 1 \\ 1 & 0 \end{bmatrix} \frac{1}{(1-f)a_{21}}. \quad (2.2.55)$$

Then,

$$\underline{\underline{X}}^{-1} \underline{\underline{R}} \underline{\underline{X}} = \begin{bmatrix} \lambda & 1 \\ 0 & \lambda \end{bmatrix}. \quad (2.2.56)$$

The rest of the solution procedure is the same as that for the case (a.2) shown above. The non-recursive solutions (2.2.46) and (2.2.47) apply for this case.

**(b.3)**  $\lambda_1 = \lambda_2$  ( $f = 1$ )

In this case, the eigenvalue is equal to  $\lambda = 0$ . Therefore, the system matrix  $\underline{\underline{R}} = \underline{\underline{0}}$ . From the general non-recursive solutions (2.2.16) and (2.2.17), the non-recursive solutions for this case can be written as

$$\underline{\underline{C}}^{(i)} = \underline{\underline{A}} \underline{\underline{\gamma}}, \quad \underline{\underline{C}}^{o(i)} = \underline{\underline{\gamma}}, \quad i = 0, 1, 2, \dots \quad (2.2.57)$$

Notice that in this case the radionuclide fractions in the transmuter core at the beginning and the end of the irradiation are independent of the cycle number  $i$ .

In summary, the formula for each radionuclide can be obtained by calculating the matrix multiplications in (2.2.40), (2.2.41), (2.2.46) and (2.2.47), resulting in

$$C_1^{(i)} = a_{11} [\beta_1 + F_1(i; \lambda_1, \lambda_2)], \quad i = 1, 2, 3, \dots, \quad (2.2.58)$$

$$C_2^{(i)} = a_{21} [\beta_1 + F_1(i; \lambda_1, \lambda_2)] + a_{22} [\beta_2 + F_2(i; \lambda_1, \lambda_2)], \quad i = 1, 2, 3, \dots, \quad (2.2.59)$$

$$C_1^{o(i-1)} = \beta_1 + F_1(i; \lambda_1, \lambda_2), \quad i = 1, 2, 3, \dots, \quad (2.2.60)$$

$$C_2^{o(i-1)} = \beta_2 + F_2(i; \lambda_1, \lambda_2), \quad i = 1, 2, 3, \dots, \quad (2.2.61)$$

where 
$$\beta_1 \equiv \frac{f}{(1-\lambda_1)(1-\lambda_2)} (\gamma_1 - r_{22}\gamma_1 + r_{12}\gamma_2), \quad \beta_2 \equiv \frac{f}{(1-\lambda_1)(1-\lambda_2)} (\gamma_2 - r_{11}\gamma_2 + r_{21}\gamma_1), \quad (2.2.62)$$

$$F_1(i; \lambda_1, \lambda_2) \equiv \begin{cases} \frac{1}{\lambda_2 - \lambda_1} [K_1(\lambda_2)\xi(\lambda_1)\lambda_1^{i-1} - K_1(\lambda_1)\xi(\lambda_2)\lambda_2^{i-1}], & \lambda_1 \neq \lambda_2, \\ \lambda^{i-2} \left[ \gamma_1 \xi(\lambda) \lambda - K_1(\lambda) \left\{ (i-1)\xi(\lambda) - \frac{f\lambda}{(1-\lambda)^2} \right\} \right], & \lambda_1 = \lambda_2 = \lambda, \end{cases} \quad i = 1, 2, 3, \dots, \quad (2.2.63)$$

$$F_2(i; \lambda_1, \lambda_2) \equiv \begin{cases} \frac{1}{\lambda_2 - \lambda_1} [K_2(\lambda_2)\xi(\lambda_1)\lambda_1^{i-1} + K_2(\lambda_1)\xi(\lambda_2)\lambda_2^{i-1}] & \lambda_1 \neq \lambda_2, \\ \lambda^{i-2} \left[ \gamma_2 \xi(\lambda) \lambda - K_2(\lambda) \left\{ (i-1)\xi(\lambda) - \frac{f\lambda}{(1-\lambda)^2} \right\} \right], & \lambda_1 = \lambda_2 = \lambda, \end{cases} \quad i = 1, 2, 3, \dots, \quad (2.2.64)$$

$$K_1(\lambda) \equiv (\lambda - r_{11})\gamma_1 - r_{12}\gamma_2, \quad K_2(\lambda) \equiv (\lambda - r_{22})\gamma_2 - r_{21}\gamma_1, \quad \xi(\lambda) \equiv 1 - \frac{f}{1-\lambda} \quad (2.2.65)$$

In (2.2.65),  $\lambda$  is a dummy variable, which is not equal to 1. These non-recursive solutions (2.2.58) to (2.2.61) are valid for the parameter ranges,  $0 < \alpha \leq 1$ ,  $0 < f \leq 1$ ,  $d_1 \geq 0$ ,  $d_2 \geq 0$ ,  $d_1 \geq p_2 \geq 0$ ,  $0 < \gamma_1 \leq 1$ ,  $0 \leq \gamma_2 < 1$ .



### 2.2.3 Asymptotic Behavior of Non-Recursive Solutions for Large Cycle Numbers

The fractions of radionuclides are dependent on the eigenvalues of the system matrix  $\underline{R}$  and the cycle number  $i$ . The eigenvalues are constant once the system parameters are constant. The above equations describe the change in the fraction of radionuclides in the transmuter along the operation of the transmutation system. The dependency on the cycle number appears as the power of the eigenvalues, and is included in the functions,  $F_1(i; \lambda_1, \lambda_2)$  and  $F_2(i; \lambda_1, \lambda_2)$  as shown in (2.2.58) and (2.2.59). If we assume that the moduli of the eigenvalues are smaller than 1, the multiple power of the eigenvalues will vanish for a large number of cycles. *i.e.*,

$$\lim_{i \rightarrow \infty} F_1(i; \lambda_1, \lambda_2) = 0, \quad \lim_{i \rightarrow \infty} F_2(i; \lambda_1, \lambda_2) = 0, \quad \text{for } |\lambda_1| < 1, \quad |\lambda_2| < 1. \quad (2.2.66)$$

Hence, as  $i$  tends to infinity, the fractions,  $C_1^{(i)}$  and  $C_2^{(i)}$ , tend to,

$$\begin{aligned} C_1^{(\infty)} &\equiv \lim_{i \rightarrow \infty} C_1^{(i)} = \beta_1 a_{11}, \\ C_1^{(\infty)} &\equiv \lim_{i \rightarrow \infty} C_1^{(i)} = \beta_1, \\ C_2^{(\infty)} &\equiv \lim_{i \rightarrow \infty} C_2^{(i)} = \beta_1 a_{21} + \beta_2 a_{22}, \\ C_2^{(\infty)} &\equiv \lim_{i \rightarrow \infty} C_2^{(i)} = \beta_2, \end{aligned} \quad \text{for } |\lambda_1| < 1, \quad |\lambda_2| < 1. \quad (2.2.67)$$

Thus, the system approaches a steady state as  $i$  tends to infinity. Although this could be observed from the numerical results by the recursive form, the non-recursive form gives clear mathematical explanation for this behavior.

## 2.3 Some Quantities of Interest

### 2.3.1 Cumulative Fractions of TRU Radionuclides in Waste

Because one of major objectives of the ATW system is to reduce the mass of TRU radionuclides in the LWR spent fuel, the amount of TRU radionuclides that are *not* recovered by the partitioning and are included in the waste stream is of special interest

At each cycle, the fraction of radionuclide  $j$ ,  $j = 1, 2$ , that is not recovered by the partitioning and is included in the waste is given by (2.1.17). For a multiple-cycle situation, for the  $i$ -th cycle, (2.1.17) can be written as

$$L_j^{(i)} = \alpha f C_j^{(i)}, \quad j = 1, 2, \quad i = 1, 2, 3, \dots \quad (2.3.1)$$

The cumulative fraction  $\bar{L}_j^{(i)}$  of radionuclide  $j$  that are included in the waste up to the  $i$ -th cycle is, therefore, written as

$$\bar{L}_j^{(i)} = f \alpha \sum_{m=1}^i C_j^{(m)}, \quad j = 1, 2, \quad i = 1, 2, 3, \dots \quad (2.3.2)$$

With (2.2.58) and (2.2.59), (2.3.2) can be written as

$$\bar{L}_1^{(i)} = f \alpha \beta_1 a_{11} i + f \alpha a_{11} \sum_{m=1}^i F_1(m; \lambda_1, \lambda_2), \quad i = 1, 2, 3, \dots, \quad (2.3.3)$$

$$\bar{L}_2^{(i)} = f \alpha (\beta_1 a_{21} + \beta_2 a_{22}) i + f \alpha \sum_{m=1}^i [a_{21} F_1(m; \lambda_1, \lambda_2) + a_{22} F_2(m; \lambda_1, \lambda_2)], \quad i = 1, 2, 3, \dots \quad (2.3.4)$$

The summation terms in (2.3.3) and (2.3.4) converge to finite values, as  $i$  tends to infinity if  $|\lambda_1| < 1$ ,  $|\lambda_2| < 1$ . The cumulative fraction  $\bar{L}_j^{(i)}$  increases as  $i$  increases due to the first term on the right side.

### 2.3.2 Cumulative Feed of TRU Radionuclides

For a multi-recycle situation, the deficit  $\Delta^{(i)}$  at cycle  $i$  is written as, by the analogy of (2.1.20),

$$\Delta^{(i)} = f - (X_1^{(i)} + X_2^{(i)}). \quad (2.3.5)$$

Furthermore, by (2.1.18),  $\Delta^{(i)}$  can be written as

$$\Delta^{(i)} = f - (1 - \alpha) f \{C_1^{(i)} + C_2^{(i)}\}. \quad (2.3.6)$$

The cumulative fraction  $\bar{S}_j^{(i)}$  of TRU radionuclide  $j$  that is supplied from the TRU storage up to the  $i$ -th cycle is written as

$$\bar{S}_j^{(i)} \equiv \gamma_j \sum_{m=1}^i \Delta^{(m)} = \gamma_j \sum_{m=1}^i \left[ f - (1-\alpha) f \left\{ C_1^{(m)} + C_2^{(m)} \right\} \right]. \quad (2.3.7)$$

By (2.3.2),

$$\bar{S}_j^{(i)} = \gamma_j \left[ f i - \frac{1-\alpha}{\alpha} \left\{ \bar{L}_1^{(i)} + \bar{L}_2^{(i)} \right\} \right]. \quad (2.3.8)$$

### 2.3.3 Cumulative Fraction of Transmutation Products in Waste

The fraction for transmutation products separated at the partitioning process for the discharged fuel at the  $i$ -th cycle is given by, from (2.1.17),

$$L_p^{(i)} = f C_p^{(i)}, \quad (2.3.9)$$

where the fraction  $C_p^{(i)}$  of transmutation products in the core at the end of the irradiation period of the  $i$ -th cycle is written as (2.1.13). But, if we utilize the relation (2.1.11),  $C_p^{(i)}$  can be written in terms of  $C_1^{(i)}$  and  $C_2^{(i)}$  as

$$C_p^{(i)} = 1 - C_1^{(i)} - C_2^{(i)}. \quad (2.3.10)$$

By (2.3.10), (2.2.58) and (2.2.59), (2.3.9) becomes

$$L_p^{(i)} = f \left[ \left\{ 1 - (a_{11} + a_{21}) \beta_1 - a_{22} \beta_2 \right\} - \left\{ (a_{11} + a_{21}) F_1(i; \lambda_1, \lambda_2) + a_{22} F_2(i; \lambda_1, \lambda_2) \right\} \right], \quad i = 1, 2, 3, \dots \quad (2.3.11)$$

Similar to (2.3.2), the cumulative fraction  $\bar{L}_p^{(i)}$  of transmutation products that are included in the waste up to the  $i$ -th cycle is written as

$$\bar{L}_p^{(i)} = f \left[ 1 - (a_{11} + a_{21}) \beta_1 - a_{22} \beta_2 \right] i - f \sum_{m=1}^i \left\{ (a_{11} + a_{21}) F_1(m; \lambda_1, \lambda_2) + a_{22} F_2(m; \lambda_1, \lambda_2) \right\}, \quad i = 1, 2, 3, \dots \quad (2.3.12)$$

By (2.3.3), (2.3.4), (2.3.8), and (2.3.12), it can be readily shown that

$$\bar{S}_1^{(i)} + \bar{S}_2^{(i)} = \bar{L}_1^{(i)} + \bar{L}_2^{(i)} + \bar{L}_p^{(i)}. \quad (2.3.13)$$

### 2.3.4 TRU Reduction Ratio

By  $\bar{L}_j^{(i)}$  and  $\bar{S}_j^{(i)}$ , the TRU reduction ratio is defined as

$$\rho_j^{(i)} \equiv \frac{\bar{L}_j^{(i)}}{\bar{S}_j^{(i)}}, \quad i = 1, 2, 3, \dots, \quad j = 1, 2. \quad (2.3.14)$$

With (2.3.3), (2.3.4), and (2.3.8), the ratios are written as

$$\rho_1^{(i)} = \frac{\alpha \beta_1 a_{11} i + \alpha a_{11} \sum_{m=1}^i F_1(m; \lambda_1, \lambda_2)}{\gamma_1 \left[ \left\{ 1 - (1-\alpha)(\beta_1 a_{11} + \beta_1 a_{21} + \beta_2 a_{22}) \right\} i - (1-\alpha) \sum_{m=1}^i \left[ (a_{11} + a_{21}) F_1(m; \lambda_1, \lambda_2) + a_{22} F_2(m; \lambda_1, \lambda_2) \right] \right]}, \quad (2.3.15)$$

$$i = 1, 2, 3, \dots, \quad j = 1, 2,$$

$$\rho_2^{(i)} = \frac{\alpha (\beta_1 a_{21} + \beta_2 a_{22}) i + \alpha \sum_{m=1}^i \left[ a_{21} F_1(m; \lambda_1, \lambda_2) + a_{22} F_2(m; \lambda_1, \lambda_2) \right]}{\gamma_2 \left[ \left\{ 1 - (1-\alpha)(\beta_1 a_{11} + \beta_1 a_{21} + \beta_2 a_{22}) \right\} i - (1-\alpha) \sum_{m=1}^i \left[ (a_{11} + a_{21}) F_1(m; \lambda_1, \lambda_2) + a_{22} F_2(m; \lambda_1, \lambda_2) \right] \right]}, \quad (2.3.16)$$

$$i = 1, 2, 3, \dots, \quad j = 1, 2.$$

As  $i$  tends to infinity, the summation terms in the numerator and the denominator of (2.3.15) and (2.3.16) approach finite values if  $|\lambda_1| < 1$ ,  $|\lambda_2| < 1$ . Therefore, the reduction ratio tends to a finite value,

$$\rho_1^{(\infty)} \equiv \lim_{i \rightarrow \infty} \rho_1^{(i)} = \frac{\alpha \beta_1 a_{11}}{\gamma_1 \left\{ 1 - (1-\alpha)(\beta_1 a_{11} + \beta_1 a_{21} + \beta_2 a_{22}) \right\}}, \quad \text{for } |\lambda_1| < 1, \quad |\lambda_2| < 1. \quad (2.3.17)$$

$$\rho_2^{(\infty)} \equiv \lim_{i \rightarrow \infty} \rho_2^{(i)} = \frac{\alpha(\beta_1 a_{21} + \beta_2 a_{22})}{\gamma_2 \{1 - (1 - \alpha)(\beta_1 a_{11} + \beta_1 a_{21} + \beta_2 a_{22})\}}, \text{ for } |\lambda_1| < 1, |\lambda_2| < 1. \quad (2.3.18)$$

Substituting the definitions (2.1.16) and (2.2.62) into (2.3.17) and (2.3.18) yields

$$\rho_1^{(\infty)} = \frac{\alpha f \exp(-d_1)}{1 - (1 - \alpha f) \exp(-d_1)}, \text{ for } |\lambda_1| < 1, |\lambda_2| < 1, \quad (2.3.19)$$

$$\rho_2^{(\infty)} = \frac{\alpha f \left\{ \frac{\gamma_1}{\gamma_2} a_{21} + \exp(-d_2) [1 - (1 - \alpha f) \exp(-d_1)] \right\}}{[1 - (1 - \alpha f) \exp(-d_1)] [1 - (1 - \alpha f) \exp(-d_2)]}, \text{ } |\lambda_1| < 1, |\lambda_2| < 1, \gamma_2 \neq 0. \quad (2.3.20)$$

It should be pointed out that the two system parameters,  $\alpha$  and  $f$ , always appear together in the above formulae. Formula (2.3.20) cannot be used for the case with  $\gamma_2 = 0$ . In that case, the feed material from the TRU storage does not contain the second-member TRU radionuclide. Because the TRU reduction ratio compares the amount of the radionuclide in the waste to that in the feed, the ratio cannot be defined for the case with  $\gamma_2 = 0$ .

If  $a_{21} = 0$ , then (2.3.20) becomes

$$\rho_2^{(\infty)} = \frac{\alpha f \exp(-d_2)}{[1 - (1 - \alpha f) \exp(-d_2)]}, \text{ for } |\lambda_1| < 1, |\lambda_2| < 1, a_{21} = 0. \quad (2.3.21)$$

Formula (2.3.21) has a form identical to that of (2.3.19), except that the parameter  $d_1$  is replaced with  $d_2$ . This indicates that, if two radionuclides in the fuel are not connected by the production of one nuclide from the other by the chain (2.1.2), then the reduction ratio at a steady state can be determined independently for each radionuclide.

If  $d_1 = d_2$  and  $a_{21} = 0$ , then  $\rho_2^{(\infty)}$  becomes identical to  $\rho_1^{(\infty)}$ . This corresponds to the one-nuclide case.

### 2.3.5 Transmutation-Product Ratio

The transmutation-product ratio is defined as that of the cumulative fraction  $\bar{L}_p^{(i)}$  of transmutation product to the cumulative TRU feed as

$$\rho_p^{(i)} \equiv \frac{\bar{L}_p^{(i)}}{\bar{S}_1^{(i)} + \bar{S}_2^{(i)}}, i = 1, 2, 3, \dots \quad (2.3.22)$$

By (2.1.1), (2.3.3), (2.3.4), (2.3.8), and (2.3.12), (2.3.22) can be written as

$$\rho_p^{(i)} \equiv \frac{[1 - (a_{11} + a_{21})\beta_1 - a_{22}\beta_2] i - \sum_{m=1}^i \{ (a_{11} + a_{21})F_1(m; \lambda_1, \lambda_2) + a_{22}F_2(m; \lambda_1, \lambda_2) \}}{[1 - (1 - \alpha)(\beta_1 a_{11} + \beta_1 a_{21} + \beta_2 a_{22})] i - (1 - \alpha) \sum_{m=1}^i [(a_{21} + a_{11})F_1(m; \lambda_1, \lambda_2) + a_{22}F_2(m; \lambda_1, \lambda_2)]}, \quad (2.3.23)$$

$i = 1, 2, 3, \dots$

As  $i$  tends to infinity, the transmutation-product ratio approaches a finite values if  $|\lambda_1| < 1, |\lambda_2| < 1$ , i.e.,

$$\rho_p^{(\infty)} \equiv \lim_{i \rightarrow \infty} \rho_p^{(i)} = \frac{1 - (a_{11} + a_{21})\beta_1 - a_{22}\beta_2}{1 - (1 - \alpha)(\beta_1 a_{11} + \beta_1 a_{21} + \beta_2 a_{22})}, \text{ for } |\lambda_1| < 1, |\lambda_2| < 1. \quad (2.3.24)$$

Substituting the definitions of parameters yields

$$\rho_p^{(\infty)} = \frac{[1 - (1 - \alpha f) \exp(-d_1)] [1 - \exp(-d_2)] + \gamma_1 \alpha f [\exp(-d_2) - \exp(-d_1) - a_{21}]}{[1 - (1 - \alpha f) \exp(-d_1)] [1 - (1 - \alpha f) \exp(-d_2)]}, \quad (2.3.25)$$

for  $|\lambda_1| < 1, |\lambda_2| < 1$ .

The two system parameters,  $\alpha$  and  $f$ , always appear together in the above formula. If  $d_1 = d_2 = d$  and  $a_{21} = 0$ , then (2.3.25) becomes

$$\rho_p^{(\infty)} = \frac{1 - \exp(-d)}{1 - (1 - \alpha f) \exp(-d)}, \text{ for } |\lambda_1| < 1, |\lambda_2| < 1. \quad (2.3.26)$$

This shows that, as  $d$  increases,  $\rho_p^{(\infty)}$  tends to unity, which physically means that the TRU radionuclide

fed to the transmuter is transmuted to the transmutation products more completely as the destruction coefficient  $d$  increases. Also, as  $\alpha f$  approaches zero,  $\rho_p^{(\infty)}$  tends to unity. With a negligibly small waste loss (represented by  $\alpha f$ ), the TRU radionuclides reside in the transmuter core for a long time, resulting in  $\rho_p^{(\infty)}$  close to unity.

### 2.3.6 The Fractional Transmutation

The fractional transmutation  $\delta_j^{(i)}$  of the member at cycle  $i$  is defined as

$$\delta_j^{(i)} = \frac{C_j^{(i-1)} - C_j^{(i)}}{C_j^{(i-1)}}, \quad j = 1, 2, \quad i = 1, 2, \dots \quad (2.3.27)$$

This fraction was used in the previous study [2], where this fraction was assumed to be constant throughout all transmutation cycles.

By substituting (2.2.58), (2.2.59), (2.2.60) and (2.2.61),  $\delta_j^{(i)}$  becomes

$$\delta_1^{(i)} = 1 - a_{11} = 1 - \exp(-d_1), \quad i = 1, 2, \dots, \quad \text{for } |\lambda_1| < 1, \quad |\lambda_2| < 1 \quad (2.3.28)$$

$$\delta_2^{(i)} = 1 - a_{22} - \frac{a_{21} [\beta_1 + F_1(i; \lambda_1, \lambda_2)]}{\beta_2 + F_2(i; \lambda_1, \lambda_2)}, \quad i = 1, 2, \dots, \quad \text{for } |\lambda_1| < 1, \quad |\lambda_2| < 1 \quad (2.3.29)$$

Thus, for the first member,  $\delta_1^{(i)}$  is constant for  $i$ , whereas for the second member,  $\delta_2^{(i)}$  is dependent on  $i$ . As  $i$  increases, the functions  $F_1(i; \lambda_1, \lambda_2)$  and  $F_2(i; \lambda_1, \lambda_2)$  vanish. Therefore, at a steady state,

$$\delta_2^{(\infty)} \equiv \lim_{i \rightarrow \infty} \delta_2^{(i)} = 1 - a_{22} - \frac{a_{21} \beta_1}{\beta_2}, \quad \text{for } |\lambda_1| < 1, \quad |\lambda_2| < 1. \quad (2.3.30)$$

Substituting (2.1.16) and (2.2.62) yields

$$\delta_2^{(\infty)} = \frac{[1 - (1 - \alpha f) \exp(-d_1)] [1 - \exp(-d_2)] - a_{21} \frac{\gamma_1}{\gamma_2} \alpha f}{[1 - (1 - \alpha f) \exp(-d_1)] + (1 - \alpha f) a_{21} \frac{\gamma_1}{\gamma_2}}, \quad \text{for } |\lambda_1| < 1, \quad |\lambda_2| < 1. \quad (2.3.31)$$

## Appendix for Chapter 2

In this appendix, it is proved that eigenvalues of the system matrix  $\underline{R}$  cannot be 1 for the assumed ranges of the system parameters,  $0 < \alpha \leq 1$ ,  $0 < f \leq 1$ ,  $d_1 > 0$ ,  $d_2 \geq 0$ ,  $d_1 \geq p_2 \geq 0$ ,  $0 < \gamma_1 \leq 1$ ,  $0 \leq \gamma_2 < 1$ ,  $\gamma_1 + \gamma_2 = 1$ .

(Proof)

The deterministic polynomial of the system matrix  $\underline{R}$  is written as

$$\lambda^2 - \text{tr}(\underline{R})\lambda + \det(\underline{R}) = 0, \quad (A1)$$

where

$$\begin{aligned} \text{tr}(\underline{R}) &= r_{11} + r_{22}, & \text{tr}(\underline{R}) &= \lambda_1 + \lambda_2, \\ \det(\underline{R}) &= r_{11}r_{22} - r_{12}r_{21}, & \det(\underline{R}) &= \lambda_1\lambda_2. \end{aligned} \quad (A2)$$

By (2.2.10),

$$\begin{aligned} \text{tr}(\underline{R}) &= (1 - \alpha f) \exp(-d_1) + (1 - f) \exp(-d_2) + \gamma_1 f (1 - \alpha) \{ \exp(-d_2) - \exp(-d_1) - a_{21} \}, \\ \det(\underline{R}) &= (1 - \alpha f)(1 - f) \exp(-d_2) \exp(-d_1). \end{aligned} \quad (A3)$$

We consider the cases for  $\lambda_1 = \lambda_2 = \lambda$  and for  $\lambda_1 \neq \lambda_2$ .

Case (i):  $\lambda_1 = \lambda_2$

In this case, there is only one eigenvalue with multiplicity equal to 2. Suppose that the eigenvalue is equal to one. Then, by (A2),

$$\text{tr}(\underline{\underline{R}}) = 2, \quad \det(\underline{\underline{R}}) = 1. \quad (\text{A4})$$

From the determinant equations shown in (A3) and (A4),

$$1 = (1 - \alpha f)(1 - f) \exp(-d_2) \exp(-d_1). \quad (\text{A5})$$

However, the right side of (A5) is always smaller than 1. Equality in (A5) cannot be satisfied by any possible combinations of the parameter values in the assumed ranges. Therefore, if there is only one distinct eigenvalue for the system matrix  $\underline{\underline{R}}$ , then it cannot be 1.

Case (ii):  $\lambda_1 \neq \lambda_2$

In this case, the system matrix  $\underline{\underline{R}}$  has two distinct eigenvalues. Suppose that one of them is equal to one, e.g.,  $\lambda_1 = 1$ . Then, the other eigenvalue  $\lambda_2$  is equal to  $\det(\underline{\underline{R}})$  by (A2). Also, by (A2),

$$\text{tr}(\underline{\underline{R}}) = 1 + \det(\underline{\underline{R}})$$

Substituting (A3) into the above equation yields

$$\begin{aligned} & (1 - \alpha f) \exp(-d_1) + (1 - f) \exp(-d_2) + \gamma_1 f (1 - \alpha) \{ \exp(-d_2) - \exp(-d_1) - a_{21} \} \\ & = 1 + (1 - \alpha f)(1 - f) \exp(-d_2) \exp(-d_1). \end{aligned} \quad (\text{A6})$$

Case (ii-a):  $0 < d_1 < d_2$

In this case,  $a_{21} = \frac{p_2}{d_2 - d_1} \{ \exp(-d_1) - \exp(-d_2) \}$ .

(A6) reduces to

$$\gamma_1 f (1 - \alpha) \left( 1 + \frac{p_2}{d_2 - d_1} \right) \{ \exp(-d_2) - \exp(-d_1) \} = \{ 1 - (1 - f) \exp(-d_2) \} \{ 1 - (1 - \alpha f) \exp(-d_1) \}. \quad (\text{A7})$$

Because  $0 < d_1 < d_2$ ,

$$\exp(-d_2) < \exp(-d_1) \quad \text{and} \quad 1 + \frac{p_2}{d_2 - d_1} > 0.$$

The left-hand side of (A7) is smaller than or equal to zero, whereas the right-hand side of (A7) is greater than zero, and smaller than or equal to 1. Equality in (A7) cannot be satisfied with any possible combinations of the system parameter values. Therefore, in this case, one of distinct eigenvalues cannot be one.

Case (ii-b):  $d_1 = d_2 = d$

In this case,  $a_{21} = p_2 \exp(-d)$ . Then, (A6) reduces to

$$-p_2 \gamma_1 f (1 - \alpha) \exp(-d) = \{ 1 - (1 - f) \exp(-d) \} \{ 1 - (1 - \alpha f) \exp(-d) \}. \quad (\text{A8})$$

The left-hand side of (A8) is smaller than or equal to zero, whereas the right-hand side of (A8) is greater than zero, and smaller than or equal to 1. Therefore, in this case, one of distinct eigenvalues cannot be one.

Case (ii-c):  $d_2 < d_1 \leq d_2 + p_2$

In this case,  $a_{21} = \frac{p_2}{d_2 - d_1} \{ \exp(-d_1) - \exp(-d_2) \}$ . (A6) reduces to (A7). Because  $d_2 < d_1 \leq d_2 + p_2$ ,

$$0 < \exp(-d_2) - \exp(-d_1) < 1 \quad \text{and} \quad 1 + \frac{p_2}{d_2 - d_1} = \frac{d_2 - d_1 + p_2}{d_2 - d_1} < 0. \quad (\text{A9})$$

The left-hand side of (A7) is smaller than or equal to zero, whereas the right-hand side of (A7) is greater than zero, and smaller than or equal to 1. Equality in (A7) cannot be satisfied with any possible combinations of the system parameter values. Therefore, in this case, one of distinct eigenvalues cannot be one.

Case (ii-d):  $d_1 > d_2 + p_2$

In this case,  $a_{21} = \frac{p_2}{d_2 - d_1} \left\{ \exp(-d_1) - \exp(-d_2) \right\}$ . (A6) reduces to (A7). Because  $d_1 > d_2 + p_2$ ,

$$0 < \exp(-d_2) - \exp(-d_1) < 1 \text{ and } -1 < \frac{p_2}{d_2 - d_1} < 0. \quad (\text{A10})$$

Rearranging (A7) yields

$$\exp(-d_1) = \frac{1 - (1-f)\exp(-d_2) - \gamma_1 f(1-\alpha) \left( 1 + \frac{p_2}{d_2 - d_1} \right) \exp(-d_2)}{(1-\alpha f) - \gamma_1 f(1-\alpha) \left( 1 + \frac{p_2}{d_2 - d_1} \right) - (1-\alpha f)(1-f)\exp(-d_2)}. \quad (\text{A11})$$

Set

$$\begin{aligned} X &\equiv \exp(-d_2), \quad 0 < X \leq 1, \\ K &\equiv (1-f) + Wf, \quad 0 < K < 1, \\ M &\equiv (1-\alpha f) - Wf, \quad M < 1, \\ L &\equiv (1-f)(1-\alpha f), \quad 0 < L < 1, \\ W &\equiv (1-\alpha)\gamma_1 \left( 1 + \frac{p_2}{d_2 - d_1} \right), \quad 0 \leq W < 1 \end{aligned} \quad (\text{A12})$$

then, (A11) becomes

$$\exp(-d_1) = g(X), \quad (\text{A13})$$

where

$$g(X) = \frac{K}{L} + \left( \frac{KM - L}{L^2} \right) \frac{1}{X - M/L}. \quad (\text{A14})$$

Notice that the case with  $\alpha = 1$  and  $f = 1$  is excluded from the present case because it makes  $\det(\underline{R}) = \text{tr}(\underline{R}) = 0$ , so that the two eigenvalues become equal to zero. We consider the range of the function for the range of  $0 < X \leq 1$  for the case with  $f \neq 1$  and the case with  $f = 1$ .

If  $f \neq 1$ , then  $\frac{dg}{dX} = \frac{-KM + L}{(LX - M)^2}$ . The denominator is positive. The numerator is smaller than or equal to zero, because in the following expression

$$-KM + L = (1-\alpha)^2 \gamma_1 f^2 \left( 1 + \frac{p_2}{d_2 - d_1} \right) \left\{ -1 + \gamma_1 \left( 1 + \frac{p_2}{d_2 - d_1} \right) \right\}$$

$(1-\alpha)^2 \gamma_1 f^2$  is greater than or equal to zero and smaller than 1. By (A10),  $\left( 1 + \frac{p_2}{d_2 - d_1} \right)$  is greater than

zero and smaller than 1. The range of  $\left\{ -1 + \gamma_1 \left( 1 + \frac{p_2}{d_2 - d_1} \right) \right\}$  is determined as, by (A10)

$$-1 < -1 + \gamma_1 \left( 1 + \frac{p_2}{d_2 - d_1} \right) < -1 + \gamma_1.$$

By the range,  $0 < \gamma_1 \leq 1$ , the above inequality becomes

$$-1 < -1 + \gamma_1 \left( 1 + \frac{p_2}{d_2 - d_1} \right) < 0.$$

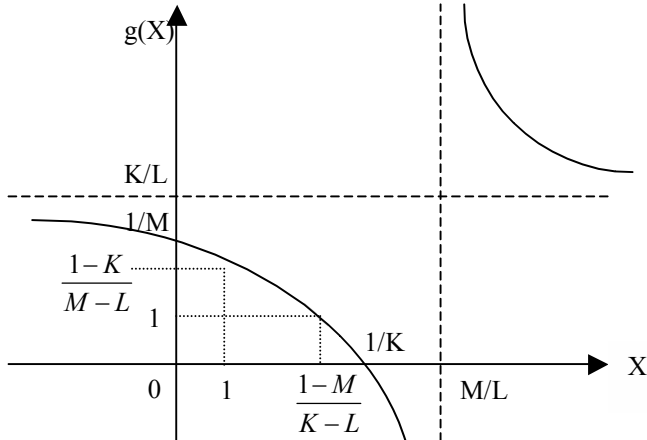
Therefore, the function,  $g(X)$ , is monotonically decreasing (if  $-KM + L < 0$ ) or constant (if  $-KM + L = 0$ ) in the range,  $0 < X \leq 1$ . But,  $-KM + L = 0$  only when  $\alpha = 0$ , for which the two distinct

eigenvalues are obtained as  $(1-f)\exp(-d_1)$  and  $(1-f)\exp(-d_2)$ . These are positive and smaller than 1. So, hereafter, we consider the case for  $-KM + L < 0$ .

The function,  $g(X)$ , has a singular point at  $X = M/L$ , and a zero at  $X = 1/K$ . The function has a value of one at  $X = (1-M)/(K-L)$ . At  $X=0$ , the function has a value of  $g(0) = 1/M$ . At  $X=1$ , the function has a value of  $g(1) = (1-K)/(M-L)$ . By (A12), the following inequalities are readily shown:

$$1 < \frac{1-M}{K-L} < \frac{1}{K} \leq \frac{M}{L}, \quad 1 < \frac{1-K}{M-L} < \frac{1}{M} \leq \frac{K}{L}. \quad (\text{A15})$$

The figure shown below depicts the function  $g(X)$ . For the range,  $0 < X \leq 1$ , the function ranges between  $1 < \frac{1-K}{M-L} < g(X) < \frac{1}{M}$ . However, to satisfy (A13), the function must have a value between 0 and 1. Thus, for this case, the system parameter values cannot be determined such that one of two distinct eigenvalues becomes 1.



If  $f = 1$ , substituting 1 into  $f$  in (A11) and (A12) yields

$$g(X) = -\frac{W}{1-W-\alpha} X + \frac{1}{1-W-\alpha}. \quad (\text{A16})$$

By substituting  $X=0$  and  $X=1$ ,

$$g(0) = \frac{1}{1-\alpha-W}, \quad g(1) = \frac{1-W}{1-\alpha-W}$$

For  $1-\alpha-W > 0$ ,  $1 < g(1) < g(0)$ . For  $1-\alpha-W < 0$ ,  $0 > g(1) > g(0)$ . In either case, the system parameter values cannot be determined such that one of two distinct eigenvalues becomes 1.

For  $1-\alpha-W = 0$ , from (A7),

$$(1-\alpha)\exp(-d_2) = 1$$

This equality holds only when  $d_2 = 0$  and  $\alpha = 0$ . But,  $\alpha = 0$  is not included in the assumed range. Therefore, the system parameter values cannot be determined such that one of two distinct eigenvalues becomes 1.

This proves the hypothesis.

### 3. NUMERICAL RESULTS AND DISCUSSIONS

For numerical illustrations based on analytical expressions obtained in the previous section, we need to determine the values of the system parameters. These are the irradiation time period,  $\hat{T}$ , the production coefficient,  $\hat{p}_2$ , of the second member, the destruction coefficients,  $\hat{d}_1$  and  $\hat{d}_2$ , of the first and second members, the waste fraction,  $\alpha$ , the core fraction,  $f$ , discharged at the end of irradiation, and the fractions,  $\gamma_1$  and  $\gamma_2$ , of the first and second members in the TRU storage. Notice that  $\gamma_1$  and  $\gamma_2$  are related by (2.1.1). The values for the system parameters given in Reference [3] are summarized in Table I. The values for  $\gamma_1, \gamma_2, \hat{d}_1, \hat{d}_2$ , and  $\hat{p}_2$  are those set for  $^{241}\text{Am}$  and  $^{237}\text{Np}$  in [3].

With the non-dimensionalization defined by (2.1.8), the number of the system parameters is reduced from seven to six, *i.e.*,  $\alpha, f, d_1, d_2, p_2$ , and  $\gamma_1$ . In Section 3.1, three cases are considered to observe the time-dependent behavior of the system. The values of the non-dimensionalized parameters are determined, based on the values shown in Table I. These are summarized in Table II. The numerical results for these three cases shown in Section 3.1 indicate that the radionuclide fractions become unchanging from one cycle to another within a relatively small number of cycles. In Section 3.2, effects of the non-dimensionalized system parameters on the steady-state TRU reduction ratio are observed.

#### 3.1 Time-Dependent Behavior

As shown in (2.2.58) to (2.2.61), the fractions for two TRU radionuclides and the transmutation product change with the cycle number,  $i$ . In this section, we make numerical calculations, utilizing the analytical expressions obtained in Section 2.2 and 2.3, to illustrate the time-dependent system behavior.

Three cases are considered as shown in Table II to observe the effects of the destruction coefficients and the production coefficient. To simplify the comparison, it is assumed that the destruction coefficients of two TRU radionuclides are identical, *i.e.*,  $d_1 = d_2 = d$ . The values for the waste fraction,  $\alpha$ , the core fraction,  $f$ , discharged at the end of irradiation, and the fractions,  $\gamma_1$  and  $\gamma_2$ , are assumed to be the same as those given in Table I for all three cases.

- In Case (a), the destruction coefficient  $d$  is assumed to be 0.05, whereas the production coefficient,  $p_2$ , for the second member is 0. This is equivalent to the case with a single radionuclide for transmutation.
- In Case (b), the destruction coefficient  $d$  is assumed to be 1. Other parameter values are the same as those for Case (a). By comparing numerical results for Case (a) with those for Case (b), effects of the destruction coefficient can be observed.
- In case (c), the production coefficient for the second member,  $p_2$ , is assumed to be 0.3, while the destruction coefficient  $d$  is 1. By comparing numerical results for Case (b) with those for Case (c), effects of the production coefficient can be observed. Notice that the eigenvalues for Case (c) are complex.

**Table I: Parameter Values Assumed in Reference [3].**

Parameters		Values
Waste fraction for TRU radionuclides	$\alpha$	0.003
Core fraction discharged	$f$	1/3
Fractions in the LWR spent fuel		
for the first radionuclide	$\gamma_1$	0.635
for the second radionuclide	$\gamma_2$	0.365
Destruction coefficient		
for the first radionuclide	$\hat{d}_1$	0.359 year <sup>-1</sup>
for the second radionuclide	$\hat{d}_2$	0.334 year <sup>-1</sup>
Production coefficient for the second radionuclide	$\hat{p}_2$	0.1 or 0.3 year <sup>-1</sup>
Irradiation time	$\hat{T}$	1/3 year



**Table II: Values for Non-Dimensionalized Parameters Used in Section 3.1, Values for Matrix Elements and Eigenvalues, and Values for Steady-State Quantities. ( $j$  in the values for eigenvalues for Case (c) is the imaginary unit.)**

		Case (a)	Case (b)	Case (c)
Non-dimensionalized system parameters				
$\alpha$			0.003	
$f$			1/3	
$\gamma_1$			0.635	
$\gamma_2$			0.365	
$d_1, d_2$		0.05		1
$p_2$			0	0.3
Matrix elements and eigenvalues				
$a_{11}$	(2.1.16)	0.95123	0.36788	0.36788
$a_{21}$		0	0	0.11036
$a_{22}$		0.95123	0.36788	0.36788
$r_{11}$	(2.2.10)	0.74954	0.28988	0.26659
$r_{12}$		-0.20074	-0.07763	-0.07763
$r_{21}$		-0.11539	-0.04462	0.05224
$r_{22}$		0.83489	0.32288	0.32288
$\lambda_1$	(2.2.20)	0.95028	0.36751	0.2947+0.0571j
$\lambda_2$		0.63415	0.24525	0.2947-0.0571j
Steady-state values				
$C_1^{(\infty)}$	(2.2.67)	0.55035	0.10317	0.09837
$C_1^{\circ(\infty)}$		0.57857	0.28045	0.26740
$C_2^{(\infty)}$		0.31634	0.05930	0.10320
$C_2^{\circ(\infty)}$		0.33256	0.16120	0.20032
$C_p^{(\infty)}$	(2.1.11)	0.13331	0.83753	0.79843
$C_p^{\circ(\infty)}$		0.08887	0.55835	0.53228
$\rho_1^{(\infty)}$	(2.3.19)	0.01913	0.000582	0.000582
$\rho_2^{(\infty)}$	(2.3.20) or (2.3.21)			0.001062
$\rho_p^{(\infty)}$	(2.3.25) or (2.3.26)	0.98087	0.99942	0.99924
$\delta_1^{(\infty)}$	(2.3.30)	0.04877	0.63212	0.63212
$\delta_2^{(\infty)}$	(2.3.31)			0.48480

### 3.1.1 TRU Radionuclide Fractions (Figure 3-1)

In Figure 3-1, the fractions of TRU radionuclides and the transmutation product in the core are plotted as functions of the cycle number,  $i$ . The formulae used for this numerical evaluation are (2.2.58), (2.2.59), (2.2.60), and (2.2.61). The fraction of transmutation product is calculated by using the relationship (2.1.11). Note that, in each figure, at the starting point ( $i = 0$ ), the fractions of the TRU radionuclides are equal to  $\gamma_1$  and  $\gamma_2$ , respectively, while the fraction for the transmutation product is zero, as specified by (2.2.5) and (2.2.6).

For Case (a), the profiles of the radionuclide fractions become unchanging after several cycles. By ocular observation, it seems that the radionuclide fractions become unchanging after 10 cycles. Hereafter, we call the regime with an unchanging profile a quasi steady state.

The difference between before and after the irradiation in the same cycle, *i.e.*, the difference between  $C_1^{\circ(i)}$  and  $C_1^{(i)}$  for the first member or between  $C_2^{\circ(i)}$  and  $C_2^{(i)}$  for the second member, is not so large due to the small value assumed for the destruction coefficient  $d = 0.05$ . As a result, the fraction of the transmutation product in the transmuter remains at around 0.1.

For Case (b), the destruction coefficient  $d$  is assumed to be 1, which is 20 times greater than that

assumed in Case (a). The difference between  $C_1^{(i)}$  and  $C_1^{(i)}$  (or between  $C_2^{(i)}$  and  $C_2^{(i)}$ ) becomes significantly greater than that observed in Case (a). Consequently, the fraction for the transmutation product after the irradiation in the transmuter,  $C_p^{(i)}$ , approaches as large as 0.837. As the transmutation coefficient increases, more TRU radionuclides are transmuted into transmutation products, which are removed from the recycle system as waste. It is also observed that the time-dependent profiles for Case (b) become unchanging within a smaller number of cycles than for Case (a). For case (b), all fractions appear to be unchanging after 5 cycles.<sup>10</sup>

For Case (c), the production coefficient  $p_2$  is assumed to be 0.3. 30% of the first member that have been transmuted becomes the second member. It is remarkable from the comparison between case (b) and case (c) that the fraction of the first member is also affected by the production of the second member. This happens because the production of the second member from the first member affects the fraction of the transmutation products, resulting in different amount of make-up when the fuel returns to the core. Due to the production of the second member, the fraction of the transmutation product for case (c) is smaller than that for case (b), whereas the fraction of the second member for case (c) is greater than that for case (b). The number of cycles necessary for the system to reach a quasi steady state seems not to be affected by  $p_2$ .

### 3.1.2 Cumulative Fractions (Figure 3-2)

Figure 3-2 shows the changes of the cumulative fractions, relative to the core, with the cycle number  $i$  for Cases (a), (b), and (c). Plotted are:

- the cumulative fractions  $\bar{L}_j^{(i)}$  of TRU radionuclide  $j$ , ( $j = 1, 2$ ) that are included in the waste up to the  $i$ -th cycle, expressed by (2.3.3) and (2.3.4),
- the cumulative fractions  $\bar{S}_j^{(i)}$  of TRU radionuclide  $j$  that is supplied from the TRU storage up to the  $i$ -th cycle, expressed by (2.3.8), and
- the cumulative fraction  $\bar{L}_p^{(i)}$  of transmutation products that are included in the waste up to the  $i$ -th cycle, expressed by (2.3.12).

Note that at each cycle, the relationship (2.3.13) holds.

These five quantities increase rapidly in the early time. After that, these quantities increase almost proportionally with  $i$ .

Because the destruction coefficient,  $d$ , assumed for Case (a) is 20 times smaller than that for Case (b), the cumulative fractions  $\bar{L}_p^{(i)}$  and  $\bar{S}_j^{(i)}$  ( $j = 1, 2$ ) are smaller nearly by the same factor for Case (a) than those for Case (b). The cumulative fractions  $\bar{L}_j^{(i)}$  of TRU radionuclides  $j$ , ( $j = 1, 2$ ) are, on the other hand, greater for Case (a) than for Case (b). More TRU radionuclides are included in the discharged fuel for Case (a) than for Case (b), resulting in more TRU radionuclides included in the waste for Case (a) than for Case (b).

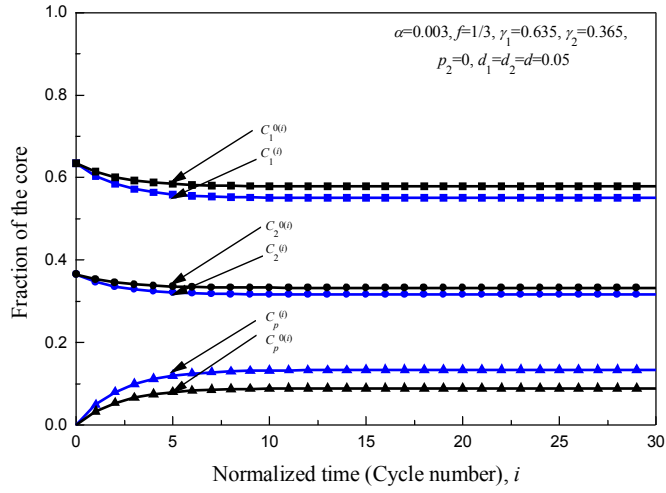
With the production of the second member from the first member, the fraction,  $\bar{L}_2^{(i)}$ , for the second member is greater for Case (c) than that for Case (b).

### 3.1.3 TRU Reduction Ratios (Figure 3-3)

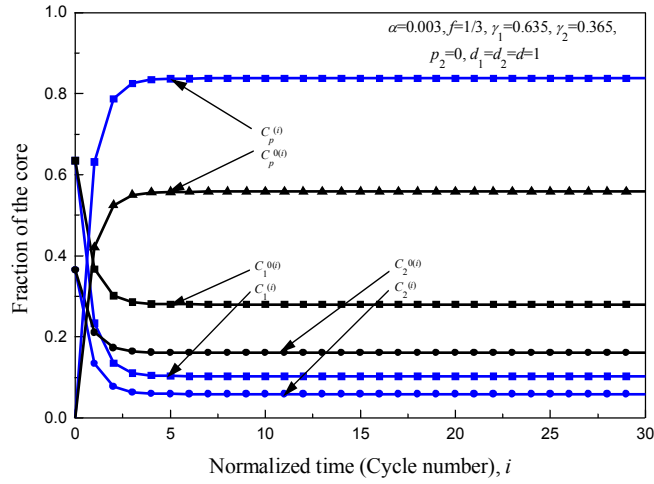
Figure 3-3 shows the change of the TRU reduction ratio,  $\rho_j^{(i)}$ , for  $j = 1, 2$ , as functions of the cycle number,  $i$ . The formulae are given by (2.3.15) and (2.3.16). For Cases (a) and (b), the ratios for the two TRU radionuclides become identical because the identical destruction  $d$  and  $p_2 = 0$  are assumed.

Comparing Case (a) with Case (b), one can see that, with the 20 times smaller  $d$ , the ratio is more than 20 times greater for Case (a) than that for Case (b). As  $i$  increases, the ratio approaches the steady-state values, which are shown in Table II. For Case (a), the steady-state value for the ratio is 0.01913, whereas that for Case (b) is 0.000582. Thus, the difference is about 33 fold. This observation implies that a greater destruction coefficient,  $d$ , is significantly effective to reduce the mass of TRU radionuclide included in the waste. Effects of the system parameters on the TRU reduction ratio will be discussed in more detail in Section 0 with the steady-state formulae, (2.3.19) and (2.3.20).

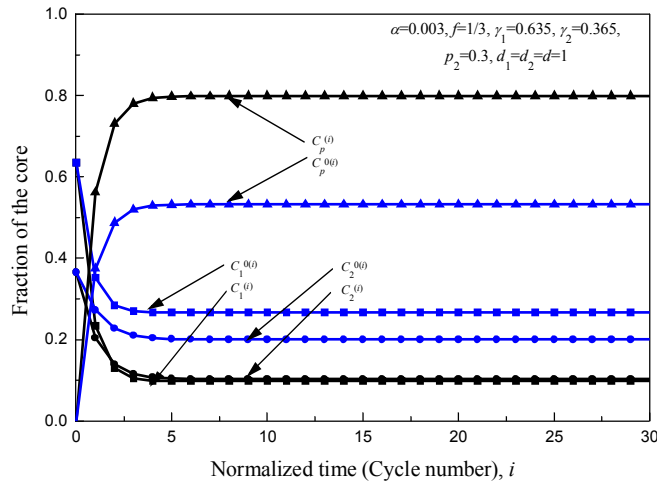
<sup>10</sup> The cycle numbers for the system to reach a quasi steady state shown in this discussion is arbitrary, and given here by crude ocular observation. More rigorous discussion should be made to distinguish the early-time transient regime and the quasi steady state regime. See Chapter 4.



Case (a)

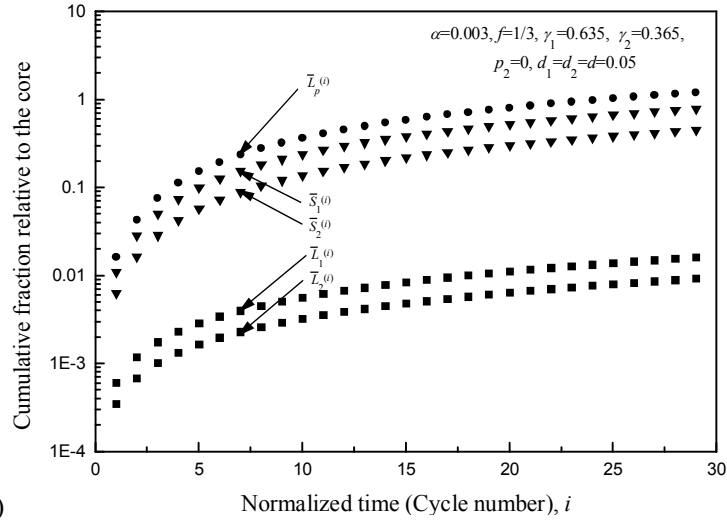


Case (b)

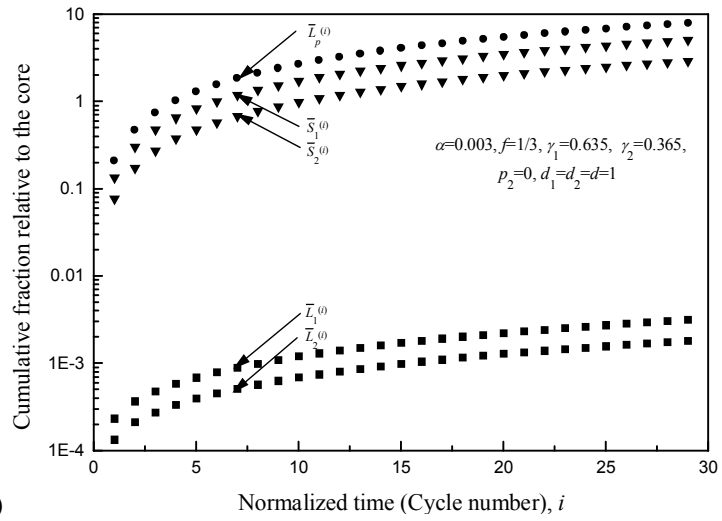


Case (c)

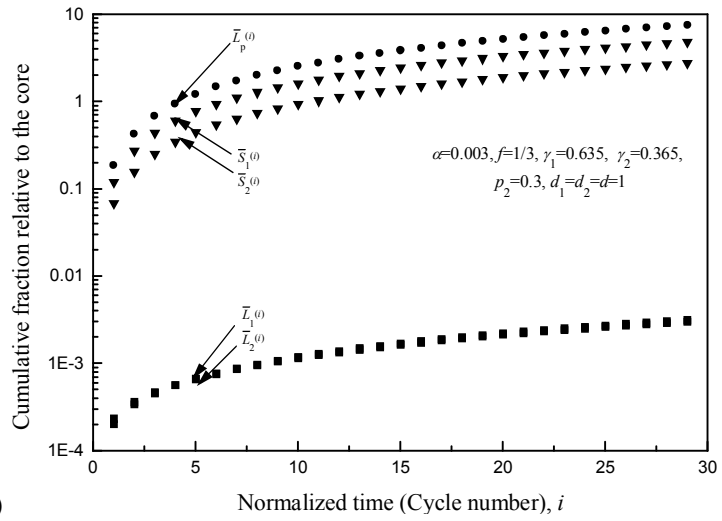
Figure 3-1: Change of radionuclide fractions in the core with the cycle number  $i$ . Cases (a) and (b) compare the effects of the destruction coefficient, whereas cases (b) and (c) compare the effects of the production coefficient.



Case (a)



Case (b)



Case (c)

Figure 3-2: Cumulative fractions relative to the core.

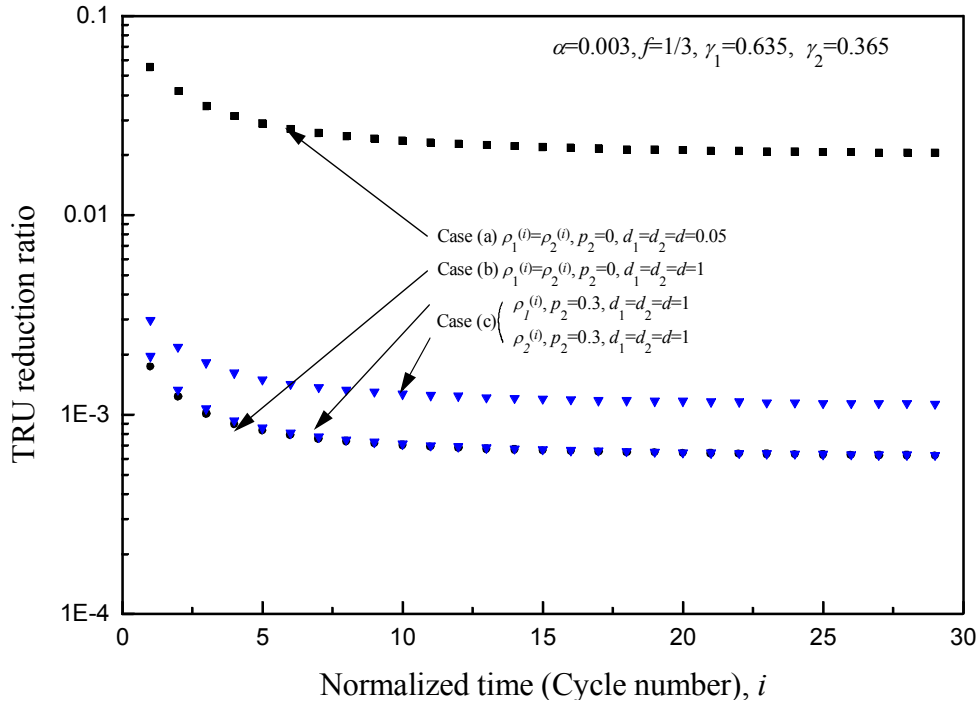


Figure 3-3: TRU reduction ratios for cases (a), (b), and (c). For cases (a) and (b), the reduction ratio is identical for both radionuclides. For case (c), the reduction ratio for the first member is the same as that for case (b).

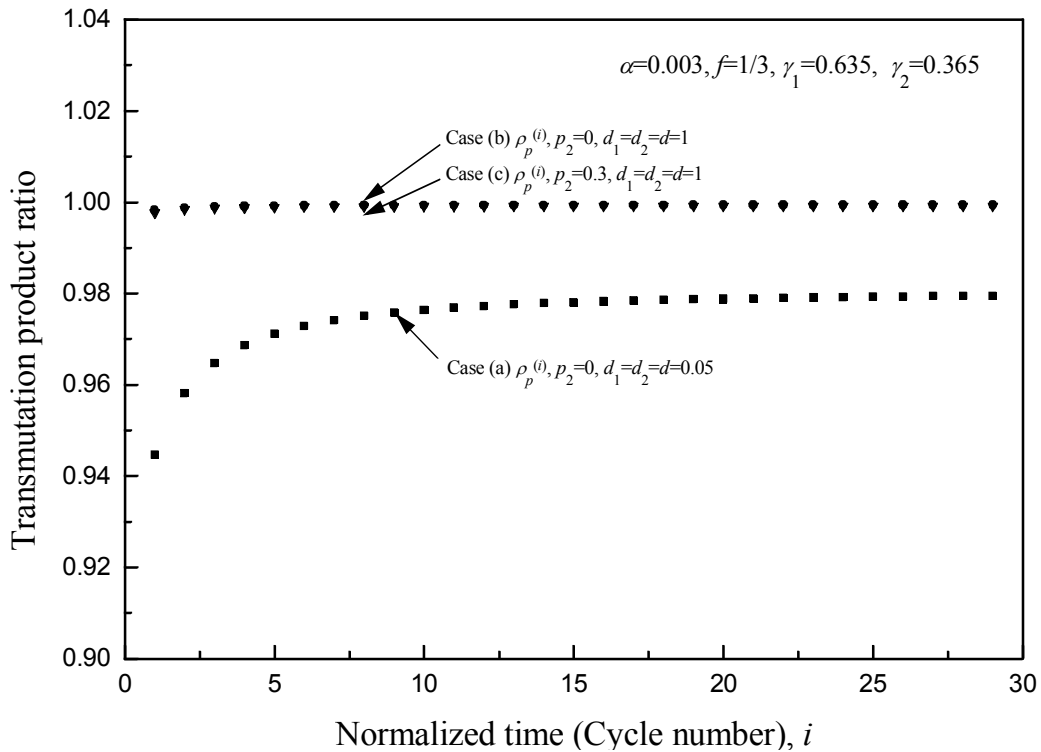
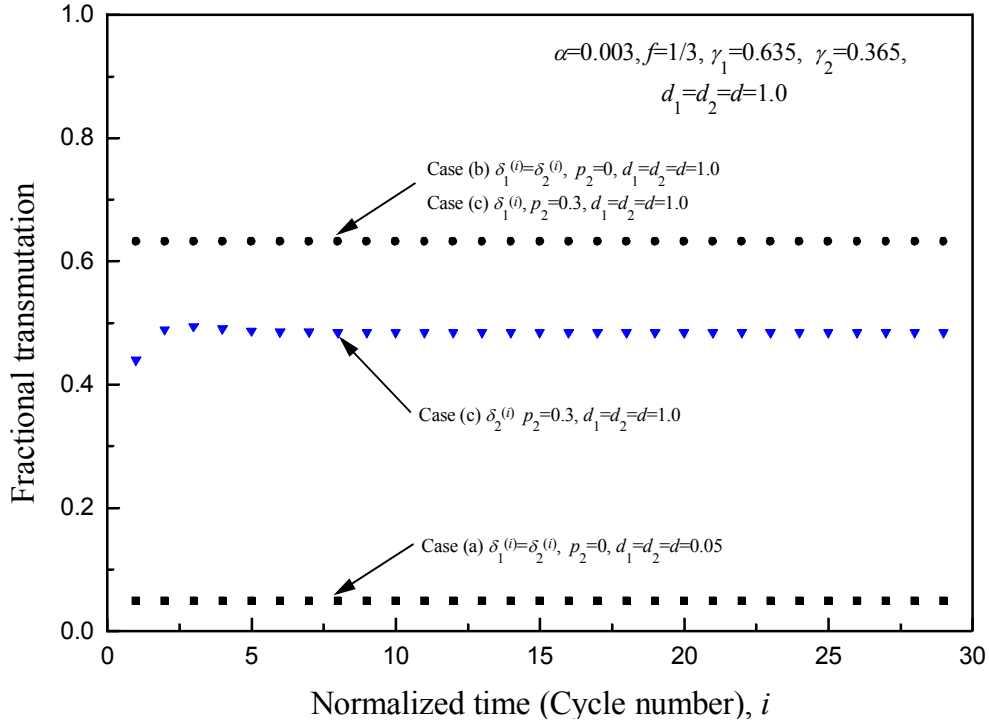


Figure 3-4: Transmutation-product ratio for cases (a), (b), and (c).



**Figure 3-5: Fractional transmutation for cases (a), (b), and (c). For cases (a) and (b), this quantity is identical for both radionuclides.**

In Figure 3-3, the values for the first member for Case (c) are nearly equal to those for Case (b). The difference between the two cases becomes smaller as  $i$  increases. At the steady state, the ratio for the first member for Cases (b) and (c) are identical, as shown in Table II and by (2.3.19), because the  $d$  value is the same.

The TRU reduction ratio for the second member for Case (c) shown in Figure 3-3 is greater than that for the ratio for the first member, because the second member is generated by the transmutation of the first member, and the same destruction coefficient,  $d$ , is assumed.

### 3.1.4 Transmutation-Product Ratio (Figure 3-4)

Figure 3-4 shows the transmutation-product ratio as a function of the cycle number  $i$ . The formula is given by (2.3.23). With the small destruction coefficient, the values for Case (a) are smaller than those for Cases (b) and (c). With  $d = 1$ , nearly 99.9% of the TRU radionuclides fed to the transmuter core have been transmuted to transmutation products, and included in the waste, whereas with  $d = 0.05$ , about 98% of the TRU radionuclides fed to the transmuter are transmuted. Comparison between Case (a) and Case (b) also shows that with a greater value for the destruction coefficient,  $d$ , the value of transmutation product approaches a steady-state value faster.

The difference between Case (b) and Case (c) is negligibly small due to a relatively large value of  $d$ , compared with that for  $p_2$ . The second member generated by the transmutation of the first member also transmutes with the relatively large value of  $d$ .

### 3.1.5 Fractional Transmutation (Figure 3-5)

Figure 3-5 shows the fractional transmutation, given by (2.3.28) and (2.3.29), as a function of  $i$ .

For Cases (a) and (b), the values for both members become identical, and independent of  $i$ , as discussed in Section 2.3.6. The fractional transmutation for Case (a) is smaller than that for Case (b), due to the smaller value of  $d$ .

For Case (c), the value for the first member is the same as that for Case (b), and independent of  $i$ . The value for the second member is dependent on  $i$ , as shown by (2.3.29), but the dependency becomes less significant as  $i$  increases.

## 3.2 Effects of System Parameters on TRU Reduction Ratio at Steady States

From the numerical results for the time-dependent behavior of the system, shown in the previous section, it is observed that the system would approach a quasi steady state within several cycles.

In this section, numerical illustrations are shown for the steady-state condition, to observe how the TRU reduction ratios are affected by the system parameters. To reduce the number of system parameters considered, the case with  $p_2 = 0$  and  $d_1=d_2$  is first observed, and then the case with  $p_2 = 0.3$  and  $d_1=d_2$  is considered to observe the effect of  $p_2$ . For the first case, there are only two independent system parameters:  $d$  and  $\alpha f$ . As observed with (2.3.19) and (2.3.21),  $\alpha$  and  $f$  always appear together. For the second case, if  $p_2$  is fixed at 0.3, there are three independent system parameters:  $d$ ,  $\gamma_1$  and  $\alpha f$ .

### 3.2.1 Case with $p_2 = 0$ and $d_1=d_2=d$

The formulae (2.3.19) and (2.3.21) are used for numerical illustration. Because  $d_1=d_2$ , these two formulae are identical. These formulae include only two independent parameters,  $d$  and  $\alpha f$ . Figure 3-6 and Figure 3-7 show the effects of these parameters on the TRU reduction ratio, one parameter at a time.

In Figure 3-6, the steady-state TRU reduction ratio is plotted as a function of  $d$ , with  $\alpha f$  as a parameter. By setting  $d_1=d_2=d$  in (2.3.19) and (2.3.21), the formula used for this numerical evaluation is written by

$$\rho_{1,2}^{(\infty)} = \frac{\alpha f \exp(-d)}{1 - (1 - \alpha f) \exp(-d)}, \text{ for } |\lambda_1| < 1, |\lambda_2| < 1. \quad (3.2.1)$$

If  $\alpha f = 1$ , then  $\rho_{1,2}^{(\infty)} = \exp(-d)$ . This corresponds to the case where the whole core ( $f = 1$  and  $\alpha = 1$ ) of the transmuter is discharged and disposed of as waste at each cycle. The reduction of the TRU radionuclide occurs only due to the transmutation in the core. Figure 3-6 indicates that the case with  $\alpha f = 1$  is the “worst” case from the viewpoint of TRU reduction<sup>11</sup>. Even in this case, if the destruction coefficient  $d$  is sufficiently large, a reduction by a factor of 1000 is still theoretically possible.

If  $0 < \alpha f < 1$ , the TRU reduction ratio becomes smaller than the case with  $\alpha f = 1$ . But, if  $d$  is small, the effect of the reduction of  $\alpha f$  becomes less significant. As  $d$  tends to 0, the ratio  $\rho_{1,2}^{(\infty)}$  tends to unity, regardless of the value of  $\alpha f$ .

This figure implies that achieving a large  $d$  is primarily important to make an effective TRU reduction. Suppose that a factor of 1000 reduction is required from the repository performance consideration. If a transmuter with  $d = 10$  is available, then the fuel after irradiation already meets the repository requirement. If a transmuter with  $d = 1$  is to be included in the system, then a partitioning process with  $\alpha f = 0.001$  is required to meet the repository requirement. If only a transmuter with  $d = 0.01$  is available, then  $\alpha f$  should be much smaller than 0.001, for which it is very unlikely that the repository requirement is met, considering that with the present partitioning technology  $\alpha f = 0.001$  would be best.

The aforementioned observation is confirmed in the next figure. Figure 3-7 shows that, if the  $d$  value is smaller than 0.01, the effect of decreasing  $\alpha f$  appears only when  $\alpha f$  is sufficiently small. For example, if  $d = 0.001$ , the TRU reduction ratio is nearly equal to 1 for  $\alpha f$  between 0.001 and 1. The ratio decreases for  $\alpha f$  between 0 and 0.001. On the other hand, if  $d = 1$ , the TRU reduction ratio decreases as  $\alpha f$  decreases almost proportionally. This parametric study indicates that, to destroy TRU radionuclides effectively by the P-T system, it is primarily important to have a large value for  $d$ .

Figure 3-8 is a contour plot for the TRU reduction ratio on the  $\log_{10}(d)$ - $\log_{10}(\alpha f)$  plane.

In the left-top half, TRU reduction effect is small, and the contour lines are nearly parallel to each other. This indicates that an increase of the coefficient  $d$  by a factor of 10 gives the same effect on the TRU reduction ratio as a decrease of the factor  $\alpha f$  by a factor of 10 (see the two solid-line arrows in the figure).

In the right-bottom half, the TRU reduction effect is significant. In the region close to the right side of the figure, the contour lines are not parallel to each other. With a value of the coefficient  $d$  ranging between 3 and 10, the TRU reduction ratio is smaller than 0.01, for any value of  $\alpha f$ . In this region, the TRU reduction ratio is more sensitive to the coefficient  $d$  than to the factor  $\alpha f$ . See the dashed-line arrows in the figure.

<sup>11</sup> For the waste reduction objective, the smaller the TRU reduction ratio is, the better the transmutation system is. How small the ratio should be should be determined in the context of performance of geologic disposal, or repository “impact.” Many previous P-T studies aimed at a reduction of TRU radionuclides in the high-level waste by a factor of 1000 or more, based on the observation for radiological toxicity of HLW.

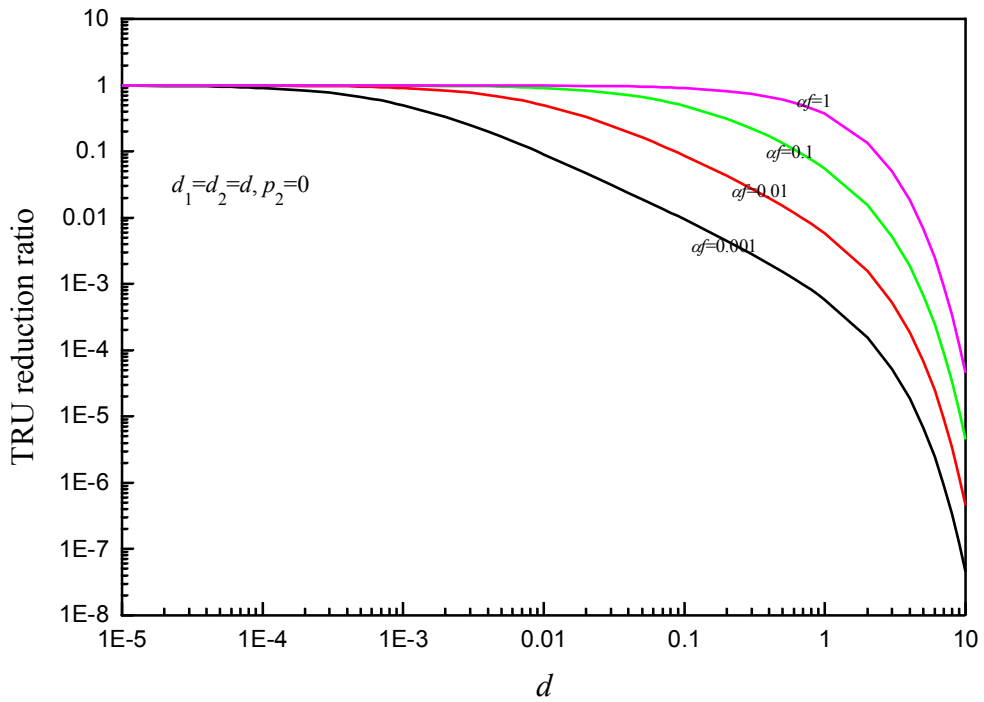


Figure 3-6: Dependency of the steady-state TRU reduction ratio on the destruction coefficient,  $d$  for  $p_2 = 0$  and  $d_1=d_2=d$ .

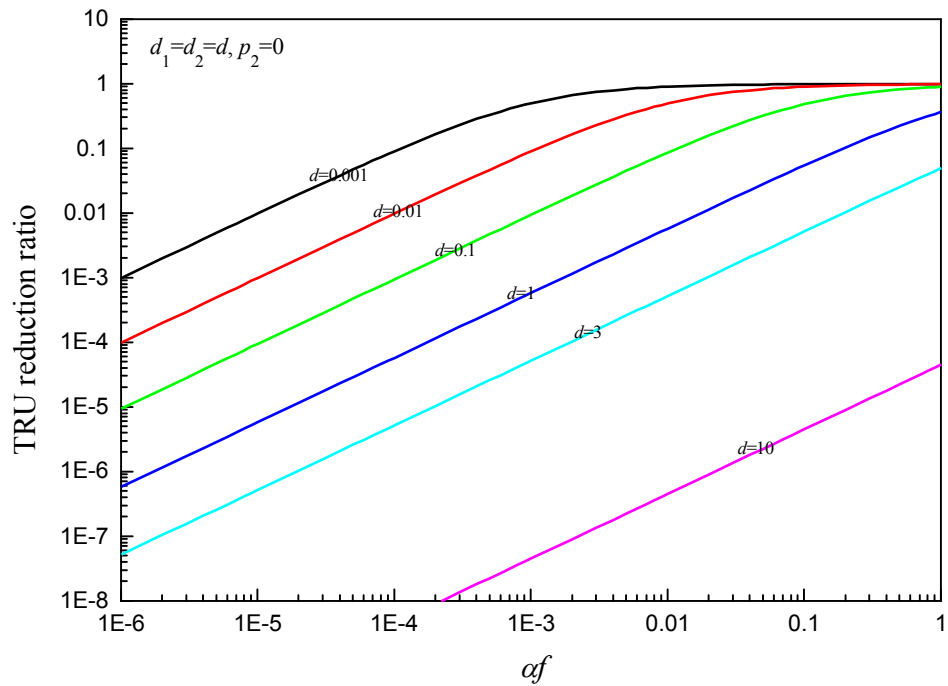
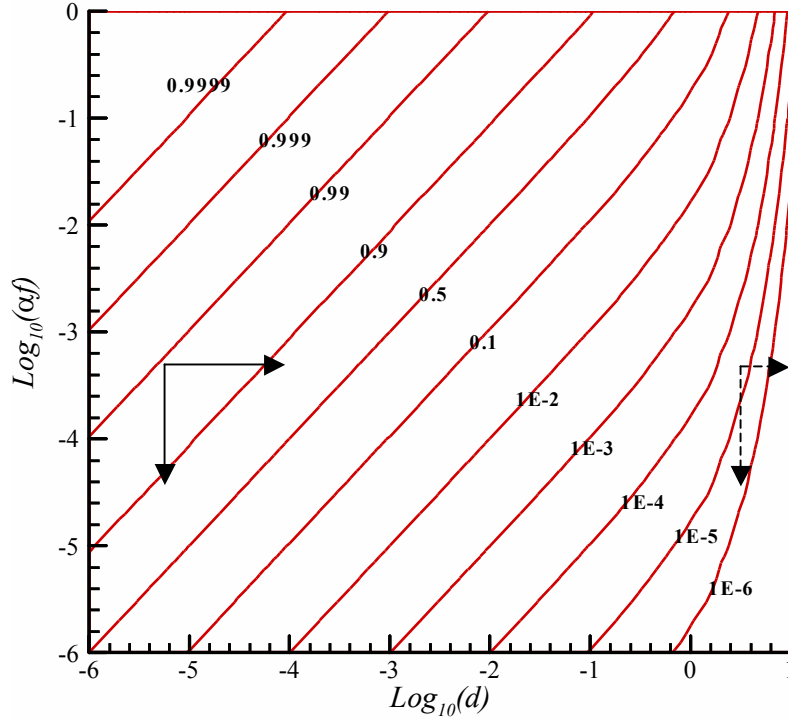


Figure 3-7: Dependency of the steady-state TRU reduction ratio on the combined parameter,  $\alpha f$  for  $p_2 = 0$  and  $d_1=d_2=d$ .





**Figure 3-8:** Contour plot for the steady-state TRU reduction ratio for  $p_2 = 0$  and  $d_1=d_2=d$ . Two solid-line arrows indicate that both an increase of  $d$  by a factor of 10 and a decrease of  $\alpha f$  by a factor of 10 give the decrease of the TRU reduction ratio from 0.99 to 0.9. The dashed-line arrows indicate that while the TRU reduction ratio is decreased from 1E-4 to 1E-5 by a decrease of  $\alpha f$  by a factor of 10 and an increase of  $d$  by a factor of 3.

### 3.2.2 Case with $p_2 = 0.3$ and $d_1=d_2=d$

Formulae (2.3.19) and (2.3.20) are utilized to numerically evaluate the steady-state TRU reduction ratios. The numerical results for the first member are the same as those shown in the previous section (Figure 3-6, Figure 3-7, and Figure 3-8). Due to the restriction (2.1.3), the numerical results in this section are obtained for  $d > p_2$ .

Figure 3-9, Figure 3-10, and Figure 3-11 are the numerical results corresponding to the preceding three figures. They show that the reduction ratio for the second member is greater than that for the first member, due to the production from the first member. It is observed that for a greater value of  $d$ , the difference between the first and second members is smaller. This is because the second member radionuclide that is generated from the first member is also transmuted effectively with a large  $d$ . The two contour plots in Figure 3-11 become similar, especially for  $\log_{10}(d)$  is greater than 0.5.

Figure 3-12 shows the effects of the fraction  $\gamma_1$  on the TRU reduction ratios at a steady state. As the fraction  $\gamma_1$  approaches unity, the steady-state TRU reduction ratio for the second member sharply increases. As  $\gamma_1$  increases, the fraction  $\gamma_2$  decreases. Thus, the contribution by the production from the first member becomes increasingly important. In some cases, the TRU reduction ratio for the second member exceeds unity. This means that more mass of the second member than that input to the P-T system comes out as the waste from the system. This situation is potentially unfavorable, especially when the second member is more toxic or more effective weapons material.

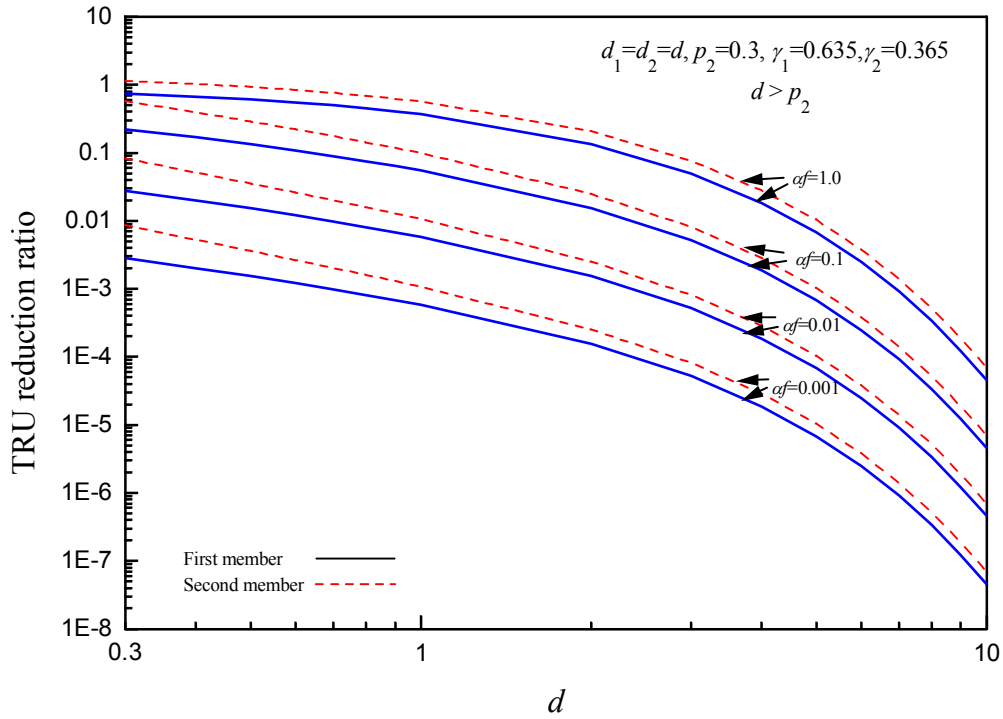


Figure 3-9: Dependency of the steady-state TRU reduction ratio on the destruction coefficient,  $d$ .

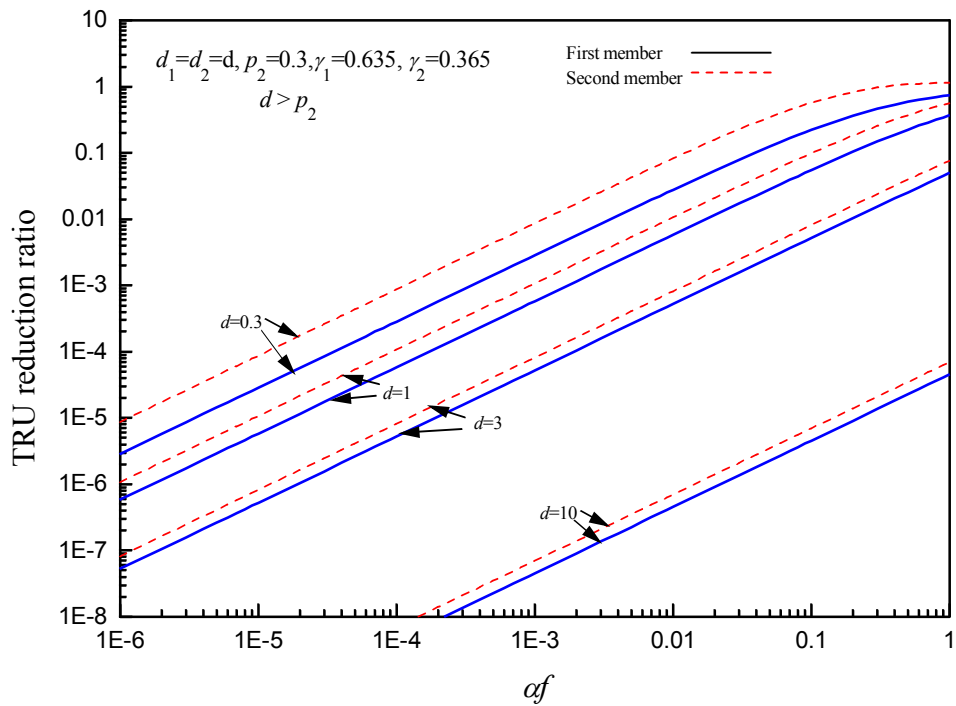


Figure 3-10: Dependency of the steady-state TRU reduction ratio on the combined parameter,  $\alpha f$ .

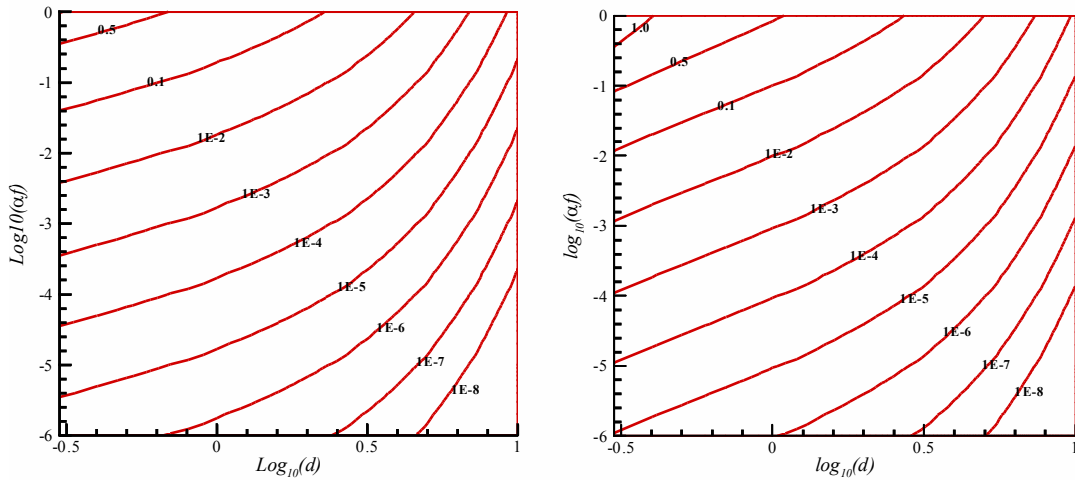


Figure 3-11: Contour plots for the steady-state TRU reduction ratios. The left figure is for the first member, whereas the right is for the second member.

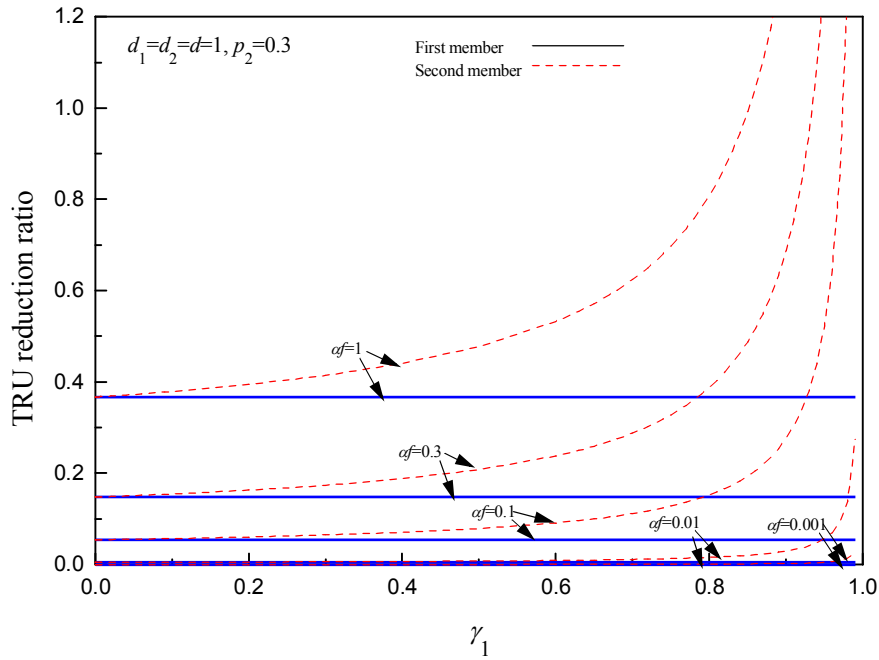


Figure 3-12: Dependency of the steady-state TRU reduction ratio on the fraction of the first member,  $\gamma_1$ .

## 4. STABILITY OF THE TWO-MEMBER SYSTEM

As shown by Eq. (2.2.66), if the moduli of the eigenvalues are less than unity, the multiple power of the eigenvalues will vanish as the cycle number  $i$  tends to infinity. As a result, the radionuclide fractions in the core before and after the irradiation become unchanging with respect to the cycle number,  $i$ , for large values of  $i$ . In this study, if the moduli of the eigenvalues are less than unity, the system is said to be *stable*. We call the state where the radionuclide fractions seem to be unchanging a *quasi steady state*. Before a quasi steady state is reached and after the start of the first cycle, the system is said to be in a transient state. The boundary between the transient state and the quasi steady state is arbitrary. In Section 3.1, numerical examples (Figure 3-3, Figure 3-5, Figure 3-6, and Figure 3-7) show that after 10 cycles or so the profiles seem unchanging. From the system operation viewpoint, it would be preferable to have a system that reaches a quasi steady state after a small number of cycles. The number of cycles the system takes before it reaches a quasi steady state is primarily determined by the magnitude of the moduli of the eigenvalues. As the magnitude of the moduli of the eigenvalues approaches zero, the system approaches its quasi steady state faster.

The questions addressed in this chapter are:

- Under what conditions, do the moduli of the eigenvalues become less than unity? (Or, when does the system become stable?)
- How do the system parameters affect the moduli of the eigenvalues?

We explore the answers to these questions for the two-member chain that has been studied in the previous chapter.

### 4.1 Upper Bounds of the Eigenvalues

The magnitude of the eigenvalue determines the stability of transmutation system. In the system with a two-member chain, two eigenvalues exist. For a stable system, the module of the largest one has to be less than one. One of the authors has established the following theorem, with which the upper bound of the eigenvalue is determined [6].

**Theorem:**

If the sum of the moduli of the elements in each column or row is less than one, the eigenvalues of matrix  $\underline{R}$  are less than one in absolute value.

**Proof:**

By the definition of the eigenvalues,

$$\underline{R}\underline{x} = \lambda\underline{x} . \quad (4.1.1)$$

where  $\underline{x}$  is an eigenvector and  $\lambda$  is an eigenvalue.

It can also be written in its elements as

$$\begin{bmatrix} r_{11} - \lambda & r_{12} \\ r_{21} & r_{22} - \lambda \end{bmatrix} \begin{bmatrix} x_1 \\ x_2 \end{bmatrix} = 0 . \quad (4.1.2)$$

For the non-trivial solution of (4.1.2), it should satisfy the following condition

$$\begin{vmatrix} r_{11} - \lambda & r_{12} \\ r_{21} & r_{22} - \lambda \end{vmatrix} = 0 , \quad (4.1.3)$$

where the determinant is applied to the matrix in (4.1.2).

The eigenvalues of matrix  $\underline{R}$  are obtained by solving (4.1.3). The magnitude of these eigenvalues can be related to the elements of the system matrix  $\underline{R}$  through (4.1.2).

By expanding (4.1.2), we get

$$\lambda x_1 = r_{11}x_1 + r_{12}x_2, \quad \lambda x_2 = r_{21}x_1 + r_{22}x_2. \quad (4.1.4)$$

Let us take absolutes on both sides of (4.1.4).

$$|\lambda x_1| = |r_{11}x_1 + r_{12}x_2|, \quad |\lambda x_2| = |r_{21}x_1 + r_{22}x_2|. \quad (4.1.5)$$

Here we utilize the following facts:

- i) the absolute values of a product is the product of the absolute values and
- ii) the absolute values of a sum is at most the sum of the absolute values of individual terms.

Hence we have relations with inequalities such that

$$|\lambda||x_1| \leq |r_{11}x_1| + |r_{12}x_2| = |r_{11}||x_1| + |r_{12}||x_2|, \quad |\lambda||x_2| \leq |r_{21}x_1| + |r_{22}x_2| = |r_{21}||x_1| + |r_{22}||x_2|. \quad (4.1.6)$$

Adding these inequalities, we have a single inequality as

$$|\lambda|(|x_1| + |x_2|) \leq (|r_{11}| + |r_{21}|)|x_1| + (|r_{12}| + |r_{22}|)|x_2|,$$

or

$$|\lambda| \leq (|r_{11}| + |r_{21}|) \frac{|x_1|}{|x_1| + |x_2|} + (|r_{12}| + |r_{22}|) \frac{|x_2|}{|x_1| + |x_2|}. \quad (4.1.7)$$

(4.1.7) shows that the magnitude of the eigenvalue must be between  $|r_{11}| + |r_{21}|$  and  $|r_{12}| + |r_{22}|$ .

If components on the right side of (4.1.7) satisfy

$$|r_{11}| + |r_{21}| < 1, \quad |r_{12}| + |r_{22}| < 1, \quad (4.1.8)$$

then (4.1.7) becomes

$$|\lambda|(|x_1| + |x_2|) < |x_1| + |x_2|,$$

or,

$$|\lambda| < 1. \quad (4.1.9)$$

Switching the element of system matrix along the diagonal leads to the transpose matrix. Both the system matrix  $\underline{R}$  and the transpose of matrix  $\underline{R}^T$ ,

$$\underline{R}^T = \begin{bmatrix} r_{11} & r_{21} \\ r_{12} & r_{22} \end{bmatrix}, \quad (4.1.10)$$

have the same eigenvalues. For the transpose, if components satisfy

$$|r_{11}| + |r_{12}| < 1, \quad |r_{21}| + |r_{22}| < 1, \quad (4.1.11)$$

the similar procedure also leads to the same conclusion as (4.1.9). This proves the theorem.

From the theorem, the upper bound of the eigenvalues can be derived by (4.1.7). The magnitude of the eigenvalue should be less than  $\nu$ , where

$$\nu = \max(|r_{11}| + |r_{12}|, |r_{21}| + |r_{22}|). \quad (4.1.12)$$

The similar procedure leads to the following expression based on the transpose matrix:

$$\nu' = \max(|r_{11}| + |r_{21}|, |r_{12}| + |r_{22}|). \quad (4.1.13)$$

The magnitude of eigenvalues is also less than the value in (4.1.13).

We have  $\nu$  and  $\nu'$  for the same eigenvalues. So, the smallest is the upper bound of the magnitude of the eigenvalues, i.e.,

$$|\lambda| < \min(\nu, \nu'). \quad (4.1.14)$$

All three cases confirm that the numerical values for the upper-bound obtained by (4.1.14) are actually greater than the moduli of the eigenvalues. In case (a), one of the four sums exceeds one. This indicates that even if the ‘‘if’’ clause of the theorem is not satisfied, a stable system can exist.

Because the Case (a) system has eigenvalues greater than those for Cases (b) and (c), the system approaches its quasi steady state more gradually than the systems for Cases (b) and (c), as observed in Figure 3-3.

## 4.2 Eigenvalues and System Parameters

In Section 4.1, the upper bound of the eigenvalues has been determined. If the upper bound determined by (4.1.14) is less than unity, then the system is stable.

In this section, we consider the other question, i.e., How do the system parameters affect the moduli of the eigenvalues?

The eigenvalues are written as (2.2.20), in terms of the elements of the system matrix,  $\underline{R}$  that are defined in terms of the system parameters by (2.2.10). As (2.2.20) shows, the formula for the eigenvalues is a complicated function of the system parameters. Instead of directly estimating the eigenvalues, we evaluate the trace of the system matrix, which is the sum of its diagonal elements. The trace of the matrix is equal to the sum of eigenvalues for a given matrix, and has a simpler form than (2.2.20).

Since we assume that the range of each eigenvalue is between 0 and 1, the addition of all eigenvalues can be minimum of zero and maximum of 2 for the case of a two-member chain. Thus,

**Table III: Upper-Bound of the Eigenvalues for Cases (a), (b), and (c).**

	Case (a)	Case (b)	Case (c)
$r_{11}$	0.74954	0.28988	0.26659
$r_{12}$	-0.20074	-0.07763	-0.07763
$r_{21}$	-0.11539	-0.04462	0.05224
$r_{22}$	0.83489	0.32288	0.32288
$ r_{11}  +  r_{12} $	0.95028	0.36751	0.34422
$ r_{21}  +  r_{22} $	0.95028	0.36750	0.37512
$v$	0.95028	0.36751	0.37512
$ r_{11}  +  r_{21} $	0.86493	0.33450	0.31883
$ r_{12}  +  r_{22} $	1.03563	0.40051	0.40051
$v^2$	1.03563	0.40051	0.40051
<i>Upper bound for <math> \lambda </math></i>	0.95028	0.36751	0.37512
$\lambda_1$	0.95028	0.36751	$0.2947+0.0571j$
$ \lambda_1 $	0.95028	0.36751	0.30022
$\lambda_2$	0.63415	0.24525	$0.2947-0.0571j$
$ \lambda_2 $	0.63415	0.24525	0.30022

$$0 \leq \lambda_1 + \lambda_2 < 2, \text{ or } 0 \leq r_{11} + r_{22} < 2. \quad (4.1.15)$$

Trace of the system matrix for a two-member chain is, from (2.2.10),

$$r_{11} + r_{22} = [1 - \alpha f - (1 - \alpha)\gamma_1 f]e^{-d_1} - (1 - \alpha)\gamma_1 f a_{21} + [1 - \alpha f - (1 - \alpha)\gamma_2 f]e^{-d_2}. \quad (4.1.16)$$

For  $p_2 \neq 0$ , and  $d_1 = d_2 = d$ ,

$$r_{11} + r_{22} = [2 - \alpha f - f]e^{-d} - (1 - \alpha)\gamma_1 f p_2 e^{-d}. \quad (4.1.17)$$

For  $p_2 = 0$  and  $d_1 = d_2 = d$ ,

$$r_{11} + r_{22} = [2 - \alpha f - f]e^{-d}. \quad (4.1.18)$$

Figure 4-1 shows the numerical values of the trace for the case with  $d_1=d_2=0.05$  and  $p_2=0$ , utilizing (4.1.18), as a function of the fraction,  $f$ . Four lines are plotted for  $\alpha = 0, 0.1, 0.5, \text{ and } 1$ . At  $f = 0$ , the value of the trace is  $2\exp(-d)$ . At  $f = 1$  and  $\alpha = 1$ , the trace is zero. The figure and (4.1.18) show that, for eigenvalues to be close to zero,  $\alpha$  and  $f$  should be close to unity, or the destruction coefficient  $d$  be large (as shown in Figure 4-2). For the case with  $f = 1$  and  $\alpha = 1$ , which can be interpreted as a once-through, direct-disposal system, the eigenvalues are equal to zero as discussed in page 12. If the  $\alpha$  value is as small as 0.003 and the fraction  $f$  is 1/3, as assumed in the ATW system, the trace becomes greater than 1.6, which implies that the system approaches its quasi steady state more slowly than the once-through, direct disposal system.

Figure 4-2 shows the profiles of the trace of the system matrix as a function of the fraction  $f$  for the case with  $d_1=d_2=d$ ,  $\alpha=0.003$ , and  $p_2=0$ , for different values of  $d$ . The figure shows that, for the small value  $\alpha = 0.003$ , the trace decreases by increasing the destruction coefficient,  $d$ . The figure also shows that with a large value of  $d$ , the trace becomes less dependent on the fraction  $f$ . The line becomes nearly horizontal for the case with  $d = 5$ . Thus, for a recycle system, it is important to achieve a large destruction coefficient for the transmuter reactor.

Figure 4-3 and Figure 4-4 show the numerical results for the case with  $p_2=0.3$ . By comparing (4.1.17) and (4.1.18), the trace for the non zero  $p_2$  is always smaller than that for  $p_2=0$ . With  $\alpha = 1$ , this difference disappears. The precursor effects become more significant if the fraction  $\alpha$  is close to zero. However, from the observation with Figure 3-3, the number of cycles necessary for the system to approach the quasi steady state does not seem so different between Case (b) and (c).

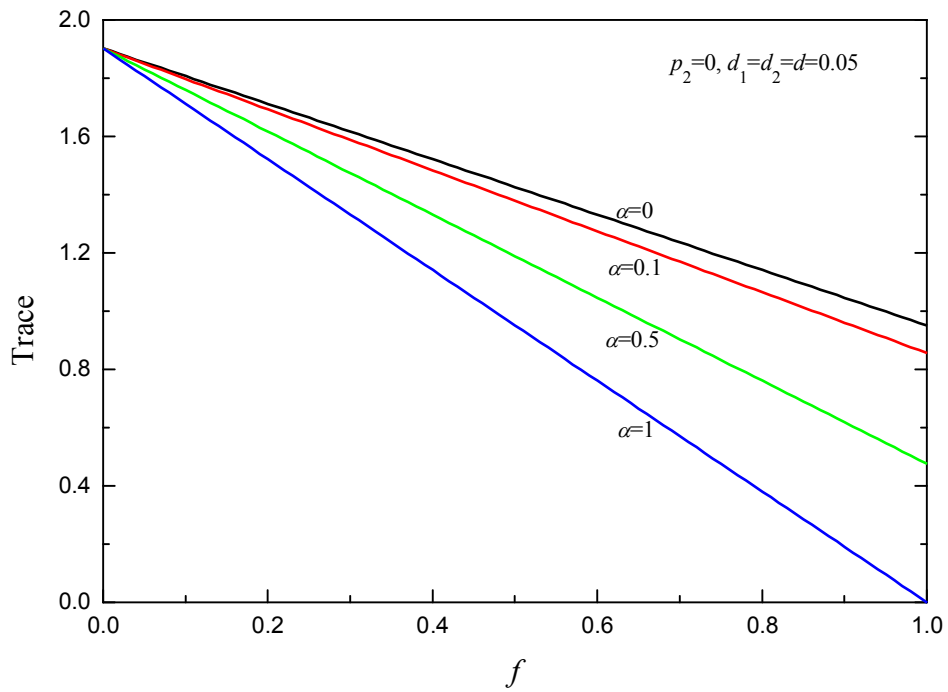


Figure 4-1: Trace of the system matrix as a function of the fraction  $f$  for the case with  $d_1=d_2=0.05$  and  $p_2=0$  for different values of  $\alpha$ , calculated by (4.1.18).

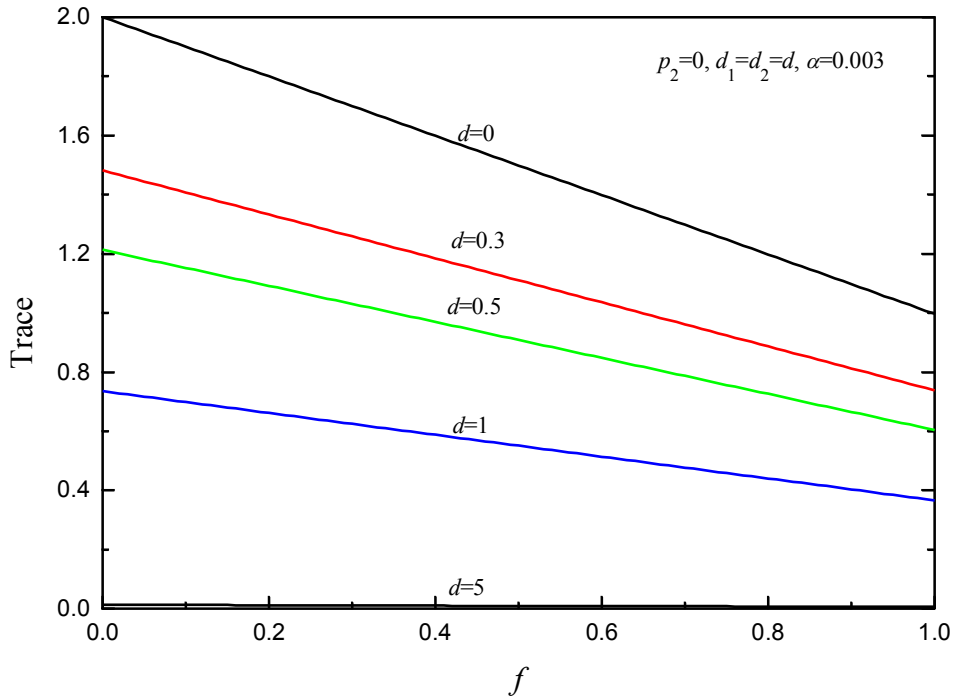


Figure 4-2: Trace of the system matrix as a function of the fraction  $f$  for the case with  $d_1=d_2=d$ ,  $\alpha=0.003$ , and  $p_2=0$ , for different values of  $d$ , calculated by (4.1.18).

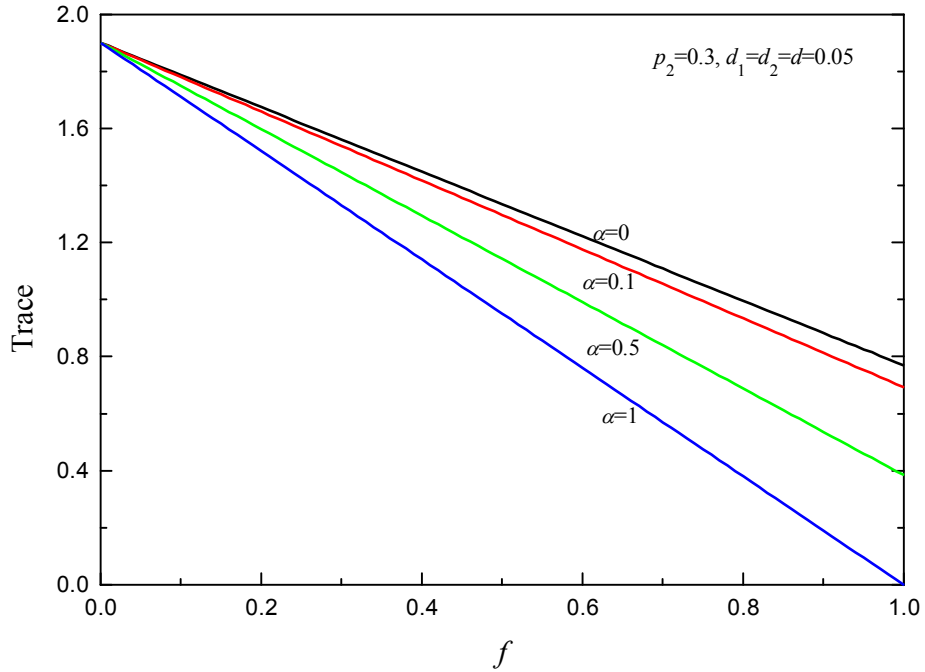


Figure 4-3: Trace of the system matrix as a function of the fraction  $f$  for the case with  $d_1=d_2=0.05$ ,  $\gamma_1 = 0.635$ , and  $p_2=0.3$  for different values of  $\alpha$ , calculated by (4.1.17).

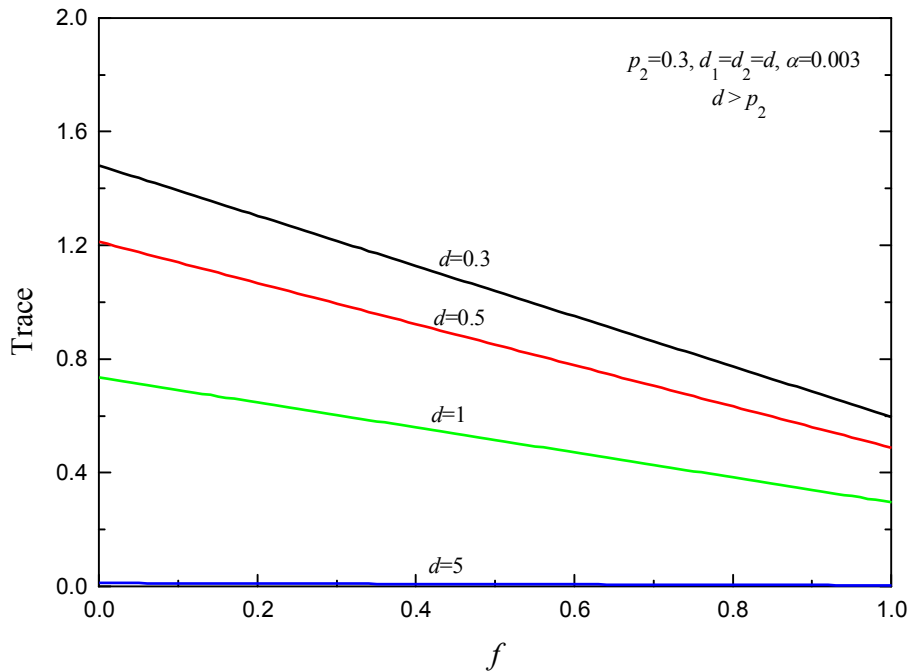


Figure 4-4: Trace of the system matrix as a function of the fraction  $f$  for the case with  $d_1=d_2=d$ ,  $\alpha=0.003$ ,  $\gamma_1 = 0.635$ , and  $p_2=0.3$ , for different values of  $d$ , calculated by (4.1.17).



## 5. CONCLUDING REMARKS

A mass flow model in an accelerator-driven transmutation system has been established for a transmutation reaction chain consisting of two TRU radionuclides. Partitioning and fuel fabrication are assumed to be done instantaneously between discharge of irradiated TRU fuel from the transmuter and installation of fabricated fuel into the transmuter.

Rate equations for transmutation reactions in the transmuter are established for the two-member chain, for which analytical solutions are written in a matrix form. Mass balance equations are written for partitioning and fuel fabrication. These are also expressed in a matrix form. The recursive solutions for the mass flow in the recycle system are obtained. Based on the recursive solutions, the non-recursive solutions for the fractions of the two TRU radionuclides in the transmuter core before and after the irradiation in the  $i$ -th cycle have been obtained by the similarity transformation.

Using the non-recursive analytical solutions, the TRU reduction ratio has been defined. This is the ratio between the amount of a TRU radionuclide included in the waste up to the  $i$ -th cycle to the amount of the same TRU radionuclide fed to the system up to the  $i$ -th cycle. This ratio is considered to be a performance measure for the transmutation system from the viewpoint of effectiveness in waste reduction.

If the moduli of the two eigenvalues of the system are less than unity, then the system is said to be stable. A stable system would reach a steady state after infinitely many recycles, where radionuclide fractions do not change from one cycle to another. A condition has been derived for the system stability, in terms of the system parameters.

With the analytical model, numerical evaluations have been made for the case with the identical destruction coefficient for the two TRU radionuclides. From the numerical results, achieving a large value of  $d$  is primarily important for effective waste reduction, because

- the system reaches a quasi steady state faster,
- from the observations with the steady-state results, the TRU reduction ratio can be decreased more effectively by increasing the destruction coefficient  $d$  than by decreasing the fraction,  $\alpha f$ , and
- the precursor effect becomes negligible, and each radionuclide can be approximately treated as a single radionuclide without precursors.

If a sufficiently large value of  $d$  ( $> 3$ ) could be realized, the fractions  $f$  and  $\alpha$  could take virtually any value between 0 and 1 to achieve an effective waste reduction (i.e., a small TRU reduction ratio). If the transmutation can be done only poorly, then the ranges of  $f$  and  $\alpha$  for effective waste reduction are more limited.

## 6. REFERENCES

- [1] For example, US Department of Energy, A Report to Congress, *A Roadmap for Developing accelerator Transmutation of Waste (ATW) Technology*, DOE/RW-0519, October 1999.
- [2] J. Ahn, M.D. Lowenthal, P.L. Chambré, E. Greenspan, W. E. Kastnberg, B.H. Park, and N. Stone, *Impact of Waste Transmutation on Repository Hazards*, International Conference on Future Nuclear Systems, Global'99, 1999.
- [3] P. L. Chambré, J. Ahn, B.H. Park, and M.D. Lowenthal, Conceptual Model for Transmutation and Recycling of Six-Member Chain with Homogenized Core, ANS Winter Meeting, 1999.
- [4] E. Greenspan and D.C. Wade, Encapsulated Nuclear Reactor Heat Source Module, *Transactions, American Nuclear Society*, **80**, 197-199, 1999.
- [5] P. L. Chambré, Notes for NE298-2 and NE299, 2000.
- [6] P. L. Chambré, Notes for NE298-2, 2001.